Published in final edited form as:
J Neurosci. 2013 February 6; 33(6): 2338–2355. doi:10.1523/JNEUROSCI.3857-12.2013.

Testosterone depletion in adult male rats increases mossy fiber transmission, LTP, and sprouting in area CA3 of hippocampus

Vanessa A. Skucas[1], **Aine M. Duffy**[1], **Lauren Harte-Hargrove**[1], **Alejandra Magagna-Poveda**[2], **Thomas Radman**[3], **Goutam Chakraborty**[1], **Charles E. Schroeder**[1,4], **Neil J. MacLusky**[5], and **H.E. Scharfman**[1,6]

[1]The Nathan Kline Institute for Psychiatric Research, Center of Dementia Research, 140 Old Orangeburg Rd., Bldg. 35, Orangeburg, NY 10962 U.S.A [2]Cantonal Hospital of Basel-Land, Institute of Pathology, Mühlemattstrasse 11, 4410 Liestal/BL Switzerland [3]Food and Drug Administration, 10903 New Hampshire Ave., Silver Spring, MD 20993 U.S.A [4]Department of Psychiatry, Columbia University, New York, NY 10032 U.S.A [5]University of Guelph, Department of Biomedical Scien, Ontario Veterinary College, Guelph, Ontario N1G 2W1 Canada [6]New York University Langone Medical Center, Departments of Child & Adolescent Psychiatry, Physiology & Neuroscience, and Psychiatry, 550 First Ave., New York, NY 10016 U.S.A

Abstract

Androgens have dramatic effects on neuronal structure and function in hippocampus. However, androgen depletion does not always lead to hippocampal impairment. To address this apparent paradox, we evaluated the hippocampus of adult male rats after gonadectomy (Gdx) or sham surgery. Surprisingly, Gdx rats showed increased synaptic transmission and long-term potentiation (LTP) of the mossy fiber (MF) pathway. Gdx rats also exhibited increased excitability and MF sprouting. We then addressed the possible underlying mechanisms, and found that Gdx induced a long-lasting upregulation of MF brain-derived neurotrophic factor (BDNF) immunoreactivity. Antagonism of Trk receptors, which bind neurotrophins such as BDNF, reversed the increase in MF transmission, excitability and LTP in Gdx rats, but there were no effects of Trk antagonism in sham controls. To determine which androgens were responsible, the effects of testosterone metabolites dihydrotestosterone (DHT) and 5α-androstane-3α,17β-diol were examined. Exposure of slices to 50 nM DHT decreased the effects of Gdx on MF transmission but 50 nM 5α-androstane-3α,17β-diol had no effect. Remarkably, there was no effect of DHT in control males. The data suggest that a Trk- and androgen receptor-sensitive form of MF transmission and synaptic plasticity emerges after Gdx. We suggest that androgens may normally be important in area CA3 to prevent hyperexcitability and aberrant axon outgrowth, but limit MF synaptic transmission and some forms of plasticity. The results also suggest a potential explanation for the maintenance of hippocampal-dependent cognitive function after androgen depletion: a reduction in androgens may lead to compensatory upregulation of MF transmission and plasticity.

Keywords

area CA3; mossy fibers; long-term potentiation (LTP); androgen; sprouting; neurotrophin; TrkB

Corresponding author: Helen E. Scharfman, Ph.D., The Nathan Kline Institute for Psychiatric Research, Center of Dementia Research, 140 Old Orangeburg Rd., Bldg. 35, Orangeburg, NY 10962, Phone: 845-398-5427, Fax: 845-398-5422, hscharfman@nki.rfmh.org or helen.scharfman@nyumc.org.

INTRODUCTION

Although the effects of estrogens on the hippocampus have been studied extensively (Spencer et al., 2008; Smith et al., 2009; Barha and Galea, 2010; Foy, 2010; Wojtowicz and Mozrzymas, 2010; Fester et al., 2011), how androgens affect the hippocampus remains poorly understood. Androgen receptors are abundant in the hippocampus (Clancy et al., 1992; Brown et al., 1995; Kerr et al., 1995; DonCarlos et al., 2003; Tabori et al., 2005; Sarkey et al., 2008), suggesting that androgens regulate hippocampal function. Moreover, there are many examples of sex differences in hippocampus [for reviews, see: (McEwen and Milner, 2007; Galea, 2008; McLaughlin et al., 2009; Mitsushima, 2011)], which also suggest a role of androgens (Becker et al., 2008; Etgen and Pfaff, 2009; Mitsushima et al., 2009). Studies examining the effects of androgens in hippocampus have, however, yielded mixed results. In rodents, testosterone administration improves hippocampal-dependent behavior in some studies (Edinger and Frye, 2004; Edinger and Frye, 2007a; Edinger and Frye, 2007 b; Frye et al., 2008) but not others (Naghdi and Asadollahi, 2004; Naghdi et al., 2005; Harooni et al., 2008). Testosterone application to hippocampal slices of adult male rats potentiates Schaffer collateral transmission in area CA1 (Smith et al., 2002), but testosterone depletion following gonadectomy (Gdx) can facilitate long-term potentiation (LTP) in area CA1 (Harley et al., 2000; Sakata et al., 2000). Testosterone administration to Gdx rats increases the number of spine synapses in stratum radiatum of area CA1 (Leranth et al., 2003), consistent with a role for androgen in maintaining normal cognitive function (MacLusky et al., 2006). However, in men, androgen ablation therapy for prostate cancer leads to few or no significant deficits in cognitive performance (Nelson et al., 2008; Alibhai et al., 2010a; Alibhai et al., 2010b; Matousek and Sherwin, 2010). The reduced levels of androgens in aging men are often considered to be a contributing factor to diseases that increase with age such as Alzheimer's disease (Fuller et al., 2007; Drummond et al., 2009; Barron and Pike, 2011; Luchetti et al., 2011), epilepsy (Herzog, 1991; Harden and MacLusky, 2004; 2005; Frye, 2006; Reddy, 2010; Stevens and Harden, 2011) and Parkinson's disease (Al Sweidi et al., 2011). However, direct evidence in support of this idea, such as prevention of these diseases by androgen therapy, is generally weak, although androgens ameliorate symptoms in some instancess (Herzog, 1991; Almeida and Flicker, 2003; Cherrier et al., 2005; Harden and MacLusky, 2005; Driscoll and Resnick, 2007).

We hypothesized that the actions of testosterone on the hippocampus might involve both positive and negative effects, which could explain previous contradictory results. This idea originated in our findings that intact male rats exhibit low levels of hippocampal BDNF immunoreactivity compared to females, primarily in the mossy fiber (MF) pathway (Scharfman et al., 2003). Therefore, androgens may normally keep BDNF protein levels relatively low, which would maintain normal excitability, but possibly limit plasticity - i.e., androgens would have positive and negative effects. In addition, this hypothesis is based on previous studies suggesting an important role for neurotrophins as mediators of gonadal steroid action (Toran-Allerand, 1984; Toran-Allerand et al., 1999) and specifically androgens and BDNF - in avian or neuromuscular systems (Ball et al., 1984; Wissman and Brenowitz, 2009; Louissaint et al., 2002; Ottem et al., 2007; Verhoveshek et al., 2010). Therefore, we asked whether testosterone regulates BDNF expression in MFs, as well as anatomical and electrophysiological indices of MF transmission and plasticity in adult male rats. Our results show, remarkably, that Gdx rats exhibit increased BDNF protein expression in the MFs and increased MF plasticity.

MATERIALS AND METHODS

Adult male rats (Charles River, Kingston, NY) were bred-in house, weaned at 21–23 days and housed (2–3/cage) with food (Purina 5001, WF Fisher, Somerville, NJ) and water *ad*

libitum and a 12 hr light:dark cycle. Chemicals were from Sigma-Aldrich unless stated otherwise. All procedures involving animals were approved by the animal care and use committee of The Nathan Kline Institute for Psychiatric Research.

I. Surgical procedures

Prior to Gdx, animals were anesthetized with 1 ml/kg ketamine-xylaxine solution (80 mg/ml ketamine hydrochloride and 12 mg/ml xyalzine hydrochloride). Bilateral Gdx was conducted as previously described (Edwards et al., 1999). In brief, a 1/2 inch midline incision of the lower abdomen was followed by removal of the testes and ligation around the vasculature adjacent to each gonad with sterile sutures (Dermalon, Henry Schein, Melville, NY). The incision was closed with wound clips (Stoelting, Kiel, WI), swabbed with betadine (Henry Schein, Melville, NY), and animals were placed over a heating pad (Homeothermic Blanket, Harvard Apparatus, Holliston, MA) until they recovered from anesthesia. Sham surgery used the same procedures, but the testes were not removed from the abdominal cavity.

For comparison of Gdx and sham rats in the Results section, animals were subjected to surgery shortly after puberty (50–60 days old). Animals were used for experiments approximately 2 weeks later to allow ample time for recovery.

II. Electrophysiology

A. Slice preparation—After deep anesthesia by isoflurane inhalation, the rat was decapitated, the brain was removed from the skull, and it was placed in ice-cold (4°C) oxygenated (95%O_2/5%CO_2) sucrose-based artificial cerebrospinal fluid (ACSF, in mM: 252.0 sucrose, 5.0 KCl, 2.4 $CaCl_2$, 2.0 $MgSO_4$, 26.0 $NaHCO_3$, 1.25 NaH_2PO_4, 10.0 d-glucose) for approximately 2 minutes. One hemisphere was glued with cyanoacrylate (Krazy Glue, Columbia, OH) to the Teflon-coated stage of a vibrating tissue slicer (Vibroslice, Stoelting) and slices (400μm–thick) were cut in the horizontal plane while immersed in 4°C ACSF. Slices were placed immediately in 100 ml of pre-oxygenated, room-temperature ACSF, and placed with a wide-bore Pasteur pipette on a nylon net of a recording chamber [modified from one previously sold by Fine Science Tools (Scharfman et al., 2001)] to provide improved flow of ACSF and increased aeration (http://www.healthresearch.org/technology-transfer/brain-and-tissue-slice-recording). Slices were perfused with oxygenated (95%O_2/5%CO_2), pre-heated (30°C) ACSF at approximately 1 ml/min by a peristaltic pump (Minpuls2, Gilson, Middleton, WI). The compartment of the recording chamber where slices were placed was maintained at 31–32°C by a temperature controller (PTCO3, Scientific Systems Design, Mississauga, Ontario). After 30 minutes, slices were perfused with NaCl-based ACSF (126.0 mM NaCl instead of sucrose). Recordings began 60 min after slices were first placed in the recording chamber and 30 min after the start of perfusion with NaCl-ACSF.

B. Recording—Similar recording procedures to those described previously (Scharfman et al., 2000; Scharfman et al., 2007; Skucas et al., 2011) were used. Recording electrodes were pulled (Model P87, Sutter Instruments, Novato, CA) from borosilicate glass with a capillary in the lumen (1.0 mm outer diameter, 0.75 mm inner diameter, World Precision Instruments, Sarasota, FL). Recording electrode were filled with NaCl-ACSF and resistances were 3–6 MΩ. Recordings were amplified (Axoclamp 2B, Molecular Devices, Sunnyvale, CA), digitized (Digidata 1440A, Molecular Devices) and acquired using pClamp (Molecular Devices). For recording sites, a depth in the slice was chosen where the maximal response was elicited, typically 50–100 μm below the surface. For laminar analysis, the exact depth was determined by a calibrated micromanipulator with precision to the nearest micron (Leica Microsystems, Buffalo Grove, IL), and was the same for all recording sites.

C. Stimulation—Monopolar stimulating electrodes were made from Teflon-coated stainless steel wire (diameter including Teflon, 75 μm; A-M Systems, Carlsborg, WA). Stimuli were controlled by a stimulus isolation unit (IsoFlex, AMPI Instruments, Jerusalem, Israel) that generated current pulses (100 μA) which were varied in duration digitally (10–250 μsec) to test different stimulus strengths. Stimuli were triggered every 30–40 sec to test basal transmission.

For stimulation of MFs, recordings were in CA3b and the stimulating electrode was placed in the subgranular zone (SGZ) at the crest of the DG (Figure 1) because this location avoided stimulation of CA3c pyramidal cell dendrites and activation of area CA3 recurrent collaterals to other CA3 pyramidal cells (Claiborne et al., 1993). The response to MF stimulation was recorded at many sites in stratum lucidum in CA3b at the onset of each experiment, to determine the location within stratum lucidum where the maximal field EPSP (fEPSP) was recorded. Other methods to confirm that the SGZ stimulus activated MFs are shown in Figure 1. Nevertheless, we cannot exclude the possibility that a pathway besides the MF pathway was activated by SGZ stimulation, e.g. the backprojecting axons of CA3 pyramidal cells that extend deep into the hilus (Scharfman, 2007).

D. LTP—LTP experiments required a stable baseline which was defined by a 15 min period when the fEPSP slope varied within 95–105% of the mean of the first 3 evoked responses. For MF plasticity, a 25 Hz, 1 sec train was triggered twice with a 5 sec interval, and stimulus strength was 50% of the strength that elicited the maximum fEPSP. For theta-burst stimulation (TBS), 10 trains of 4 half-maximal stimuli at 100 Hz were triggered 200 ms apart. fEPSPs were normalized to the average of the 15 min baseline.

E. Data analysis

1) fEPSP: Slope was defined as the slope between two points: the start of the fEPSP and the peak. When a fiber volley preceded a fEPSP, the first point of the fEPSP slope measurement was immediately after the fiber volley. This definition of slope was chosen because the fEPSPs in Gdx rats often had an irregular rising phase, making the maximal slope difficult to measure (Figure 9A2). fEPSP amplitude was defined as the difference between the pre-stimulus baseline and the peak of the fEPSP. Paired pulse facilitation (PPF) was defined as the measurement of the second response divided by the measurement of the first response. Latency was measured from the middle of the stimulus artifact, which was 10–285 μsec in duration, to the onset of the initial negative deflection representing the rising phase of the fiber volley (for latency to the fiber volley) or the onset of the rising phase of the fEPSP [for latency to fEPSPs (Skucas et al., 2011)].

2) Population spike amplitude: The amplitude of the population spike was defined as the difference between the pre-stimulus baseline and the peak of the population spike (Scharfman, 1997). Care was taken to record the population spike at a site in stratum pyramidale where it was maximal, which typically was on the border of the pyramidal cell layer and stratum oriens [analogous to area CA1; (Scharfman et al., 2003)] rather than a site close to stratum lucidum, where the population spike can be recorded, but is not the site where it is maximal.

3) Current source density (CSD): CSD analysis was conducted using field potential recordings that began at the border of the alveus with stratum oriens in area CA3b and perpendicular to the CA3 pyramidal cell layer, ending in stratum lacunosum-moleculare at a location that was adjacent to the lateral tip of the superior blade of the DG (Figure 1). Recordings were approximately 25 μm apart and the same depth in the slice, typically 50 μm. Intervals between sites were monitored using a dissecting microscope (Stemi SV6,

Zeiss, Thornwood, NY). The one dimensional CSD profile was calculated offline using Matlab (Mathworks, Natick, MA) by deriving the second spatial derivative of the local field potential recordings using a 3-point formula. The CSD represents the transmembrane sink and source currents that generate the recorded field potential profile.

III. Immunocytochemistry

A. Perfusion and processing—Following deep anesthesia (urethane, 4 g/kg, i.p), animals were perfused through the aorta with 4% paraformaldehyde (pH 7.4) as previously described (Scharfman et al., 2002). Brains were left in the skull overnight at 4°C and removed the next day for dynorphin immunocytochemistry. They were post-fixed in 4% paraformaldehyde at 4°C and cut on a vibratome into 50 μm-thick sections. For BDNF immunocytochemistry, the brains were removed after perfusion-fixation and placed in 2% paraformaldehyde at 4°C for 2 hrs. They were cryoprotected by immersion in 30% sucrose dissolved in 0.1 M phosphate buffer. Sections (40 μm thick) were cut on a cryostat (Minotome Plus, International Equipment Company, Needham Heights, MA) the next day. Sections were processed that day, as described in C, below.

The antibody to dynorphin $B_{1–13}$ (kindly provided by Dr. Teresa Milner) has been used previously to evaluate the MF pathway (Pierce et al., 1999). The polyclonal antibody to BDNF (kindly provided by Amgen-Regeneron Partners) has also been used previously and shown robust BDNF immunoreactivity (ir) in the MF pathway (Conner et al., 1997; Yan et al., 1997; Scharfman et al., 2002; Scharfman et al., 2003). The monoclonal antibody to BDNF was used because previous studies have shown that staining with this antibody led to a qualitatively similar pattern of BDNF-ir as the polyclonal antibody (Scharfman et al., 2007). Notably, processing sections in the absence of the primary antibody failed to produce MF BDNF-ir.

B. Immunocytochemistry - Dynorphin—Sections were processed with a polyclonal antibody to dynorphin B made in rabbit (Pierce et al., 1999), using free-floating sections that were initially washed twice (5 min each) in 0.1 M TRIS buffer (pH 7.6) and treated with 1% H_2O_2 made in 0.1 M TRIS buffer (pH 7.6; 30 min). Sections were then washed in 0.1 M TRIS buffer (pH 7.6; 5 min) and treated with 0.25% Triton X-100 dissolved in 0.1 M TRIS buffer (TRIS A; 10 min), followed by 0.25% Triton X-100 and 0.005% bovine serum albumin (BSA) in 0.1 M TRIS buffer (TRIS B; 10 min). Sections were then treated with 10% normal goat serum diluted in TRIS B for 45 min. Sections were subsequently washed in TRIS A (10 min) followed by TRIS B (10 min) and incubated in antisera (1:1000; diluted in TRIS B) for 24 hrs on a rotating shaker. The next day, sections were treated with TRIS A (10 min) followed by TRIS B (10 min) and then incubated for 45 min with a biotinylated secondary antibody against rabbit IgG made in goat (1:400, Vector Labs, Burlingame, CA). Sections were washed in TRIS A (10 min), then 0.25% Triton X-100 and 0.005% BSA in 0.5 M TRIS buffer (TRIS D; pH 7.6; 10 min), and finally incubated for 1 hr in avidin-biotin horseradish peroxidase complex diluted in TRIS (ABC Standard kit, 1:1,000; Vector Labs). Immunoperoxidase labeling was developed in diaminobenzidine tetrahydrochloride (DAB; 50 mg/100 ml 0.1 M TRIS buffer) with 200 mg D-glucose, 0.3 mg glucose oxidase and 40 mg ammonium chloride, and then washed three times (5 min each) in 0.1 M TRIS buffer (pH 7.6). Sections were mounted on subbed slides, allowed to dry overnight, and then dehydrated in a series of ethanol solutions (70%, 5 min; 95%, 5 min, 100%, 10 min, 100%, 10 min), cleared in xylene (10 min) and coverslipped with Permount (Fisher Scientific; Pittsburgh, PA). The sections were viewed on a brightfield microscope (BX51, Olympus of America, Hauppague, NY) and photographed using a digital camera (Retiga 2000R, Q Imaging, Surrey, UK) using ImagePro (Media Cybernetics, Bethesda, MD). To allow

comparisons in the figures, micrographs of sections from different experimental groups were taken using the same light and camera settings.

C. Immunocytochemistry - BDNF—Sections were first washed in 0.05 M potassium phosphate buffered saline (KPBS, pH 7.3) and then treated with 0.5% H_20_2 in KPBS for 30 min. After a 5 min wash in KPBS, sections were incubated in 10% normal goat serum for the polyclonal antibody (10% horse serum for the monoclonal antibody), plus 1% BSA and 0.25% Triton X-100 in KPBS for 20 min. Sections were incubated in antisera [polyclonal: 1:30,000; (Scharfman et al., 2002; Scharfman et al., 2003); monoclonal: 1:1000; Sigma-Aldrich (Scharfman et al., 2007)] in 1% BSA and 0.25% Triton X-100 in KPBS for 48 hrs at 4°C and subsequently rinsed 10 times (10 min each) in 0.25% BSA and 0.025% Triton X-100 in 0.01 M KPBS. Sections were then incubated in a biotinylated secondary antibody against rabbit IgG made in goat (1:400; Vector) for the polyclonal antibody [or biotinylated secondary antibody against mouse IgG made in horse (1:400; Vector) for the monoclonal antibody] and 1% BSA and 0.025% Triton X-100 in KPBS for 1 hr, followed by ABC (ABC Standard kit; 1:1,000; Vector) in 1% BSA in KPBS for 1 hr. Sections were rinsed in KPBS followed by TRIS buffer, and reacted with DAB using methods identical to those described above for dynorphin, except 10 mM $NiCl_2$ was added to the DAB solution.

D. Data analysis—Quantification of immunocytochemical data used ImagePro (Media Cybernetics, Bethesda, MD). The same light settings were used for all procedures. For measurement of BDNF in the MF plexus in stratum lucidum, a square region of interest (approximately 50μm^2) was placed over the terminal field at the border of CA3a with CA2, where immunoreactivity was greatest (Scharfman et al., 2003, Scharfman et al., 2007; Figure 9H1). Three measurements (spanning the terminal field of the MFs; Figure 9H1) of the gray scale value (scale: 0–255; for the purposes of this analysis, 0 was defined as white and 255 was defined as black) were made for a given section and averaged. Three measurements were also made of the area in stratum radiatum beside the region of interest, where immunoreactivity was weak. The average of the three measurements in stratum radiatum was subtracted from the average of the three measurements in stratum lucidum to give the final gray scale value for a given section. The procedure was repeated for two other sections at a similar septotemporal level. The average value from the three sections was used as the best estimate for that animal. A similar procedure was used to determine if dynorphin-ir in stratum lucidum was increased or decreased in Gdx rats compared to sham rats.

To determine if mossy fiber sprouting occurred, a different method was employed: a region of interest was drawn around the MF plexus of CA3a in stratum lucidum and stratum oriens in the section with the most widespread MF sprouting in stratum oriens (Figure 9G1). This region of interest was then used as a template for all sections to measure the mean gray scale value within the region of interest. The template was moved to stratum radiatum to measure the background (Figure 9G1), which was subtracted.

IV. Pharmacology

A. Administration of drugs to hippocampal slices—Dihydrotestosterone (Sigma-Aldrich, St. Louis, MO) and 5α-androstane-3α, 17β-diol (Adiol; Sigma-Aldrich) were dissolved in 100% ethanol as a 1M stock solution and stored at 4°C; the stock solution was diluted in NaCl-ACSF on the day of the experiment to reach the final concentration (50 nM). K252a (LC Labs, Woburn, MA) was dissolved in dimethylsulfoxide (DMSO, Sigma-Aldrich) as a 1M stock solution and stored at 4°C. It was diluted in NaCl-ACSF on the day of the experiment to reach the final concentration (300 nM). TrkB-IgG (R&D Systems, Minneapolis, MN), control IgG (R&D Systems), and 2-(2, 3-dicarboxycyclopropyl)-glycine (DCG-IV; Tocris Bioscience, Bristol, UK) were dissolved in 0.9 % NaCl, stored at 4°C as a

concentrated stock solution (1 mM) and diluted in NaCl-ACSF on the day of use. Testosterone and placebo time-release pellets (25 mg/pellet, 21 day release; #A-151 and C-111 respectively, Innovative Research of America, Sarasota, FL) were stored at room temperature in the dark. The testosterone dose was sufficient to replace normal serum testosterone levels (Figure 2F3).

B. Hormone-replacement—A 1/4 inch incision was made between the shoulder blades immediately after gonadal removal or sham treatment, while the animal was still anesthetized. A 1/8 inch-diameter pellet was inserted under the skin. Sterile sutures were used to close the incision.

Testosterone ELISA was conducted to determine circulating levels of testosterone. Trunk blood was collected in 15 ml centrifuge tubes at the time of death, and placed at room temperature for 20–30 min. Serum was separated by centrifugation (3,000 RPM, 15 min, 23°C) and frozen (−20°C) until use. A testosterone ELISA was performed using methods provided by the manufacturer (Mouse and Rat Testosterone Kit, Calbiochem, Gibbstown, NJ). Details are provided elsewhere (Chakraborty et al., 2012).

V. Statistics

Data are expressed as mean ± standard error of the mean. The p criterion was 0.05. No more than 2 slices were used for a given animal. Student's t-tests were two-tailed and conducted using Microsoft Excel 2007 (Microsoft, Redmond, WA). Fisher's exact test, χ^2 test, ANOVA, Repeated Measures ANOVA (RMANOVA), Analysis of Covariance (ANCOVA) and non-parametric Kruskal-Wallis ANOVA were performed using Prism (GraphPad, San Francisco, CA). When reporting the results of ANOVA or RMANOVA, interactions between factors are reported in the Results only in those cases where they were statistically significant. For parametric ANOVA, where there was inhomogeneity of variance, which was determined by Bartlett's test (Prism), data were log-transformed prior to statistical analysis (Zivin and Bartko, 1976).

RESULTS

I. MF transmission is increased in Gdx rats

A. Recording procedures to study MF transmission—We first confirmed that our stimulation and recording procedures evoked responses that were mediated by MFs in adult male rats that were the same age as those that would be used for experiments (approximately 2 months old). As shown in Figure 1A–C, a stimulating electrode was placed at the crest of the DG in the SGZ, with recording electrodes in stratum lucidum of area CA3b. fEPSPs had the characteristics previously reported for MF transmission: 1) short latency to onset of the fEPSP (<4 msec), consistent with monosynaptic transmission, 2) robust paired pulse facilitation (Salin et al., 1996; Kamiya et al., 2002; Scott et al., 2008; Cosgrove et al., 2009), and 3) blockade by 1 μM DCG-IV, a metabotropic glutamate receptor subtype II agonist that blocks MF transmission [Figure 1D–F; (Yoshino et al., 1996)]. Another characteristic, a fiber volley prior to the fEPSP, occurred if stimulus strength was sufficiently strong (Figure 1E, black arrow).

Laminar analysis of the response to stimulation in CA3b showed that the fEPSP recorded in stratum lucidum was followed by a later fEPSP that was only recorded in stratum radiatum, and reversed polarity in the pyramidal cell layer (Figure 1D1–E1). CSD analysis (Figure 1D2–E2) showed a short latency sink in stratum lucidum and a longer latency sink in stratum radiatum, suggesting a monosynaptic fEPSP corresponding to activation of MFs, followed by a disynaptic fEPSP reflecting activation of recurrent collaterals of pyramidal

cells in stratum radiatum. The field potentials recorded in stratum lucidum and the cell layer were reduced >90% by DCG-IV (1 μM; n=8 slices, 3 rats; Figure 1F). Notably, 1 μM DCG-IV had no detectable effect on fEPSPs evoked by Schaffer collateral stimulation, recorded in stratum radiatum of CA1 (2 slices from 2 sham controls; fEPSP slope 30 min after DCG-IV: 99.4% of pre-DCG-IV baseline).

A small fEPSP in stratum radiatum remained after DCG-IV, (Figure 1F2), which could be due to the fact that DCG-IV did not block the response entirely. It is also possible that activation of CA3 pyramidal cell axons in the hilus (Scharfman, 2007) led to activation of recurrent collaterals to area CA3 pyramidal cell dendrites in stratum radiatum. For these reasons, the term “MF fEPSP” is used below to refer only to short latency fEPSPs recorded in stratum lucidum. “Recurrent fEPSP” is used below to refer only to the long latency fEPSPs recorded in stratum radiatum. It should be noted that the term “MF LTP” is used with caution below, because we can not rule out a possible contribution of the recurrent collateral pathway during LTP induction.

B. MF fEPSPs are increased in Gdx rats—For the comparisons of MF fEPSPs between Gdx and sham rats, animals had surgery at ages that were not different (Gdx: 68.4 ± 2.4 days old; sham: 57.2 ± 3.6 days old; n=10 slices from 8 rats/group; Student’s t-test, p=0.973), and hippocampal slices were made at similar delays after surgery (Gdx: 14.5 ± 1.6 days; sham: 13.6 ± 1.0 days; n=10 slices from 8 rats/group; Student’s t-tests, p=0.736). As shown in Figure 2A, MF fEPSPs were largest in Gdx rats (n=10 slices, 8 rats/group). There was a significant effect of Gdx on the input-output relation for fEPSP slope (two-way RMANOVA; F (1,198) 5.710; p=0.028; Figure 2B) and a significant interaction between treatment and stimulus strength (F (11,198) 2.566; p=0.005) with significantly larger fEPSP slopes in Gdx rats at all stimulus strengths except the two weakest intensities (Student’s t-tests, p<0.05; Figure 2B). Results were similar for amplitude; there was a significant effect of Gdx (two-way RMANOVA; F (1,198) 66.086; p<0.0001) and an interaction between Gdx and stimulus strength (F (11,198) 14.986; p<0.0001), with fEPSPs from Gdx rats greater in sham rats at all stimulus strengths except the weakest stimuli (Student’s t-tests, p<0.05).

When fiber volleys were measured, there was no significant effect of Gdx on the input-output relation by two-way RMANOVA (F (1,198) 0.722; p=0.407; Figure 2C). However, ANOVA based 4-parameter linear regression analysis (Scharfman et al., 2007) indicated that fiber volley amplitudes in Gdx rats were significantly higher than those for sham-operated controls (F (1,28) 18.92; p<0.001).

Gdx rats exhibited a greater MF fEPSP slope for a given fiber volley amplitude (Figure 2D). Excluding the MF fEPSPs elicited at the two weakest intensities (where fiber volleys were not present), the slope of the relation was significantly greater for Gdx rats (Linear regression analysis; F (1,17) 11.486; p=0.004; Figure 2D).

Although fEPSPs were larger in Gdx rats, there were no differences in latencies. First we measured the latency to onset of the peak of the maximal fiber volley and found that there were no significant differences between experimental groups (Gdx: 1.96 ± 0.33 msec; sham: 2.34 ± 0.26 msec; Student’s t-test; p=0.370; Figure 2E1). Then we measured the latencies to onset of MF fEPSPs; both minimal and maximal fEPSPs were measured because latency varies depending on the stimulus strength (latency is longest when stimuli are weak). There were no differences between fEPSPs of Gdx and sham rats when stimuli were minimal (35 μsec; Gdx: 3.84 ± 0.38 msec; sham: 3.81 ± 0.23 msec; Student’s t-test, p=0.952; Figure 2E2), and no differences in the maximal fEPSPs (Gdx: 3.38 ± 0.28 msec; sham: 3.36 ± 0.12 msec; Student’s t-test, p=0.957).

To confirm that effects of Gdx were due to a reduction in serum levels of testosterone, we determined whether testosterone replacement to Gdx rats blocked effects of Gdx on MF transmission. For this purpose, a time-release pellet of either testosterone or placebo was inserted subcutaneously at the time of surgery (Figure 2F1). There were four experimental groups: Gdx rats treated with a testosterone pellet (10 slices, 5 rats), Gdx rats that received a placebo pellet (12 slices, 6 rats), untreated Gdx rats (27 slices, 17 rats), and untreated sham controls (16 slices, 10 rats). MF fEPSPs were tested approximately 2 weeks after surgery. There were differences between the four groups (one-way ANOVA; F (3,64) 2.668; p=0.015), with smaller fEPSP slopes in Gdx animals that received testosterone compared to Gdx rats treated with placebo (Student's t-test, p=0.008; Figure 2F2). MF fEPSPs of Gdx animals that received placebo were not significantly different from fEPSPs of untreated Gdx rats (Student's t-test, p=0.651), and there were no significant differences between Gdx rats that received testosterone and untreated sham controls (Student's t-test, p=0.702; Figure 2F2).

To confirm that serum testosterone levels were restored by testosterone pellets, testosterone was measured by ELISA from trunk blood collected at the time of euthanasia. Gdx rats that were untreated or treated with placebo had very low testosterone levels; those thatwere below the lower limit of the assay were assigned the lower limit for their testosterone value (0.10 ng/ml; Figure 2F3). There were significant differences between the four experimental groups (Kruskal-Wallis statistic, 32.584, p<0.0001; Figure 2F3). Circulating testosterone levels in Gdx rats treated with testosterone (8.08 ± 1.4 ng/ml; n=5 rats) were significantly greater than Gdx rats treated with placebo (0.16 ± 0.04 ng/ml; n=6; Dunn's multiple comparisons test, p>0.05; Figure 2F3). However, Gdx rats treated with testosterone were not significantly different from untreated sham controls (6.52 ± 0.75 ng/ml; n=10; p>0.05; Figure 2F3). The mean value for serum testosterone of Gdx rats treated with placebo was not significantly different from Gdx rats that were untreated (0.19 ± 0.09 ng/ml; n=6; p>0.05; Figure 2F3). These data confirmed that Gdx reduced serum testosterone to a negligible level and testosterone treatment increased it to levels that were normal for the strain and age of rats that were used.

II. Paired pulse facilitation, PTP and LTP are increased in Gdx rats

Paired pulse facilitation (PPF) of MF fEPSPs was greater in Gdx rats than sham controls (Figure 3). PPF was tested using using half-maximal stimulation and a 40 msec interstimulus interval, because these are parameters where PPF is typically robust (Scharfman, 1997; Scharfman et al., 2003; Scharfman et al., 2007). PPF was significantly greater in slices from Gdx rats compared to sham controls (Gdx: 166.8 ± 3.2%; n= 15 slices, 12 rats; sham: 121.0 ± 3.2%; 14 slices, 12 rats; Student's t-test, p=0.006).

We also evaluated PPF in additional rats (Gdx: 10 slices, 7 rats; sham: n= 10 slices, 6 rats) using a range of stimulus strengths, because PPF has not been evaluated in detail at the ages we used, raising the possibility that PPF in sham rats might have been underestimated using a half-maximal stimulus. There was no significant difference in PPF across stimulus strengths in sham rats (one-way ANOVA; F (11,95) 0.096; p=0.880). PPF in Gdx rats was significantly greater than sham rats at two stimulus strengths in the middle of the input-output relation (two-way RMANOVA; F (11,154) 7.907; p=0.014; Student's t-tests, p<0.05 for 110 and 135 μsec; Figure 3A2).

Next, PPF was evaluated using a range of interstimulus intervals (10, 20, 30, 40, 60, 80, 100, 150, 200 msec; Gdx: 10 slices, 9 rats; sham: 12 slices, 7 rats) with a half-maximal stimulus strength. As shown in Figure 3B, Gdx influenced PPF (two-way RMANOVA; F (1,160) 21.560; p<0.001) with a significant interaction between interstimulus interval and effect of

Gdx (F (8,160) 3.453; p=0.001). PPF was greater in Gdx rats when interstimulus intervals were intermediate (30, 40, or 60 msec; Student's t-tests, p<0.05; Figure 3B1–2).

To examine PTP and LTP, we planned to use TBS, but several slices from Gdx rats exhibited spreading depression (SD) in response to TBS (described further below). Therefore, LTP was induced using two 25 Hz trains, 1 sec in duration, 10 sec apart; a similar procedure (25 Hz, 1 sec or 25 Hz, 5 sec) has been shown to elicit MF LTP in 18–25 day-old Wistar rats (Kwon and Castillo, 2008), which we confirmed in 30 day-old Sprague-Dawley rats (147.7 ± 6.2%; n=3 slices from 3 rats). As shown in Figure 3C1, Gdx rats exhibited LTP but sham rats did not (presumably due to their age; Gdx: 169.1 ± 20.7%; n= 9 slices, 8 rats; sham: 88.3 ± 14.1%; n= 8 slices, 7 rats; Student's t-test, p=0.008). Both groups exhibited robust PTP but Gdx rats had greater PTP (two-way RMANOVA for the first 3 minutes after LTP induction; F (1,140) 9.231; p=0.009; Student's t-test, p<0.05; Figure 3C2).

III. Gdx increases MF-evoked field potentials recorded outside stratum lucidum

Responses to MF stimulation were also recorded in the pyramidal cell layer to evaluate the extent that an increase in MF transmission led to enhanced pyramidal cell output, reflected by an increase in the population spike amplitude (Figure 4A1–2; Gdx: 17 slices, 12 rats; Sham: 12 slices, 6 rats). An input-output curve for the population spike showed that there was a significant effect of Gdx (two-way RMANOVA; F (1,108) 4.737; p=0.038; Figure 4A2). There was an interaction between surgical status (Gdx vs. sham) and stimulus strength (F (4,108) 3.749; p=0.007), with a significant increase in population spike amplitude in Gdx rats at the highest stimulus intensities (Student's t-tests, p<0.05; Figure 4A2).

PPF of the population spike was greater in Gdx rats (half-maximal stimulus intensity; 40 msec interstimulus interval; Gdx: 137.8 ± 2.3%; n=18 slices, 13 rats; sham: 109.1 ± 1.9%; n=11 slices, 7 rats; Student's t-test, p=0.040; Figure 4B–C). When multiple stimulus strengths were compared in a subset of these slices (Gdx: 10 slices, 7 rats; sham: 7 slices, 6 rats), two-way RMANOVA showed that there was an interaction between surgical treatment (Gdx or sham) and stimulus strength (F (3,42) 3.257; p=0.031) with PPF in slices from Gdx rats greater at the lowest intensity (Student's t-test, p<0.05) but not higher intensities (Student's t-test, p>0.05; Figure 4B2).

PPF was also evaluated using a range of interstimulus intervals and a half-maximal stimulus strength (Gdx: 12 slices, 8 rats; sham: 10 slices, 6 rats). Two-way RMANOVA showed that there was an interaction between surgical treatment and interstimulus interval (F (1,140) 4.072; p=0.033) with significantly greater PPF in Gdx rats at 40 and 60 msec interstimulus intervals (Student's t-tests, p=0.016, p=0.028, respectively; Figure 4C1–2). There were no significant differences between Gdx and sham rats at the short interstimulus intervals, when paired pulse inhibition typically occurs (10 or 20 msec intervals; Student's t-tests, p=0.162, p=0.220 respectively; Figure 4C1–2). Therefore, Gdx rats had greater PPF of the population spike but there was no effect on paired pulse inhibition.

Another cohort of rats was used to determine whether the delayed fEPSP recorded in stratum radiatum (referred to as the "recurrent fEPSP" below) was affected by Gdx. As shown in Figure 4D, recurrent fEPSP slopes were increased in Gdx rats (17 slices, 14 rats) compared to sham controls (16 slices, 14 rats). The input-output relation was significantly different (two-way RMANOVA; F (1,341) 8.095; p=0.008), and there was an interaction between surgical pre-treatment and stimulus strength (F (11,341) 3.269; p<0.001) with recurrent fEPSPs of Gdx rats greater than sham at all stimulus strengths except the two lowest intensities (Student's t-tests, p<0.05; Figure 4D2). The lack of a significant effect at low stimulus intensities is consistent with the idea that recurrent fEPSPs required strong

intensities of stimulation, so that pyramidal cells would reach threshold for action potential generation, and activate their recurrent collaterals.

The latencies to onset of the recurrent fEPSP were not affected by Gdx. The recurrent fEPSP that was evoked by a weak stimulus (a 35 μsec stimulus) had a 5.68 ± 0.16 msec latency to onset in slices from Gdx rats and latency was 5.69 ± 0.18 msec in slices from sham rats (Student's t-test; p=0.965). The latencies to onset of the maximal recurrent fEPSP were not different either (Gdx: 5.02 ± 0.11; sham: 5.05 ± 0.13; Student's t-test, p=0.852).

PPF of the recurrent fEPSP slope (half-maximal stimulus, 40 msec interstimulus interval) was significantly greater in Gdx rats (120.7 ± 6.7%, n=15 slices, 11 rats; sham: 98.3 ± 7.0%; n=10 slices, 9 rats; p=0.034).

IV. Dihydrotestosterone (DHT) sensitivity of MF transmission and plasticity in Gdx rats

A. MF fEPSPs of Gdx rats are reduced by DHT—Testosterone is metabolized in the brain to dihydrotestosterone (DHT), a potent agonist at the androgen receptors, which are present in MFs of the adult male rat (Tabori et al., 2005). Therefore, we determined whether a deficiency in DHT was the reason for the differences in MF transmission between Gdx and sham rats. We also determined if one of the metabolites of DHT, 5α-androstane 3α,17β-diol (Adiol) would have effects on MF fEPSPs, because several studies suggest a potent effect of Adiol to enhance the actions of GABA at $GABA_A$ receptors (Frye et al., 2001; Edinger et al., 2004; Frye and Edinger, 2004; Frye et al., 2004; Reddy, 2004b; a; Edinger and Frye, 2005; Kaminski et al., 2005; Frye et al., 2010; Reddy and Jian, 2010).

MF stimulation in normal ACSF was initially tested for a 10 min baseline period to confirm that fEPSP slope was stable (Figure 5A1). Then slices were exposed to vehicle (0.0005% ethanol in ACSF) and the responses that were recorded 30 min later were compared to the baseline to confirm that vehicle had no detectable effect. Next, slices were exposed for 30 minutes to Adiol at a concentration that induced near-maximal potentiation of $GABA_A$ receptors in whole-cell recordings from CA1 pyramidal neurons (50 nM; (Reddy and Jian, 2010). Afterwards, ACSF containing 50 nM DHT was applied for 30 min.

As shown in Figure 5A2, MF fEPSPs of Gdx rats declined during exposure to DHT. One-way RMANOVA in Gdx rats showed that there was a significant change in fEPSP slope during the experiment (F (3,15) 21.786; p<0.001) with fEPSP slope decreasing to 72.3 ± 3.2% of control following DHT, significantly different from responses recorded before DHT (Paired t-test, p=0.017). However, there were no significant effects of vehicle or Adiol (Paired t-tests, p>0.05). In sham rats, there was no effect of either DHT or Adiol (one-way RMANOVA; F (3,11) 0.316; p=0.814; Figure 5B).

These experiments suggested that DHT decreased MF transmission but Adiol did not. However, the effect of DHT could have been due in part to pretreatment with Adiol, because Adiol can be converted back to DHT in the brain (Chetyrkin et al., 2001). It is also possible that altering GABAergic transmission by pre-exposure to Adiol might affect subsequent responses to DHT, even though Adiol by itself had no measurable effect. To test this possibility, slices from Gdx rats were treated with 50 nM DHT immediately after the baseline (Figure 5B1). DHT reduced the slope of the fEPSP to 74.8 ± 5.6% of control (n=5 slices, 5 rats; Paired t-test, p=0.004; Figure 5B2). In contrast, there were no effects of Adiol after it was added (immediately after the baseline; n= 3 slices, 3 rats; Figure 5C1–2), and there was no significant effect of DHT in slices from sham controls (n=4 slices, 4 rats; Paired t-test, p=0.384; data not shown).

To confirm that DHT had effects on MF-evoked population spikes, and also that DHT inhibited MF transmission at multiple stimulus strengths, recordings were made in the the pyramidal cell layer of Gdx rats in response to three intensities of MF stimulation: ~30%, 50% and 100% of the maximum. Comparisons were made between baseline and 30 min after the onset of treatment (vehicle, n=4 slices, 4 rats; DHT, n=4 slices, 4 rats). There was a significant effect of DHT (RMANOVA; $F(1,12)$ 40.17; $p<0.001$), with amplitudes lower after DHT exposure at all stimulus intensities (Bonferroni's tests, $p<0.05$). There was a significant interaction between stimulus strength and treatment ($F(2,12)$ 8.72; $p=0.005$).

In summary, DHT reduced fEPSPs in Gdx rats but Adiol did not, and there were no significant effects of any of the steroids in slices from sham controls. The results suggest that an androgen receptor-sensitive component of MF transmission emerges after Gdx.

B. MF LTP in Gdx rats is reduced by DHT—Because a DHT-sensitive component of synaptic transmission emerged after Gdx, we tested the DHT-dependence of LTP in Gdx rats. After a 15 min baseline period, slices were exposed to 50 nM DHT or vehicle (Figure 5D). LTP was induced 15 min later, the time when DHT began to exert its effects in the experiments described above. In slices where the fEPSPs declined within 15 min, an adjustment in stimulus intensity was made so that the train used to induce LTP would be half-maximal. Exposure to DHT continued until 15 min after LTP induction and then drug-free buffer was used for the remainder of the experiment. LTP was reduced in DHT-treated slices compared to slices from Gdx rats treated with vehicle (Gdx + DHT, 85.5 ± 10.1%; Gdx + vehicle, 135.1 ±13.1%; Student's t-test; $p=0.020$; Figure 5D).

Figure 5E compares LTP in slices from Gdx rats that were pre-exposed to DHT before LTP was tested, Gdx rats pretreated with vehicle, slices from Gdx rats that had no pretreatment, and slices from sham rats that were untreated. LTP in DHT-treated slices from Gdx rats was comparable to LTP in slices of untreated sham rats (Student's t-test, $p=0.475$); LTP in vehicle-treated slices of Gdx rats was similar to untreated slices of Gdx rats (Student's t-test, $p=0.565$).

PTP was also reduced by DHT (Figure 5E). Compared to vehicle-treated slices, fEPSP slopes in the first 3 min after LTP induction were significantly reduced by DHT (two-way RMANOVA ($F(1,45)$ 5.291; $p=0.047$; Figure 5F).

In summary, a DHT-sensitive component of MF PTP and LTP was present in slices from Gdx rats. Sham rats did not exhibit LTP, so the DHT-sensititve component of PTP and LTP was only evident in Gdx rats.

V. Hyperexcitability in Gdx rats

While recording in the pyramidal cell layer of Gdx rats, increased excitability was detected in a subset of slices (Figure 6). The increase in excitability was manifested in several ways. For example, a single MF stimulus could evoke >1 population spike whereas in sham rats there was only 1 population spike/stimulus. Also, there were small (~1 mV) spontaneous field potentials in slices of Gdx rats when recordings were made in the pyramidal cell layer, and more unit activity than sham rats (Figure 6A).

Another sign of abnormal excitability in slices from Gdx rats was SD in response to repetitive MF stimulation (Figure 6B). When SD followed TBS stimulation of the MFs, it did so rapidly (within seconds; Figure 6B). SD episodes were stereotypical: they were composed of an initial phase where small (~1 mV) spontaneous population spikes occurred and a second phase where there was a negative shift in the DC potential which peaked at −14 to −16 mV within approximately 15 seconds of the onset of spontaneous activity

(Figure 6B). Subsequently there was a recovery of the DC potential within approximately 5 minutes (Figure 6B). During the recovery, no response to MF stimulation could be elicited even in response to the highest stimulus strength.

The first type of hyperexcitability, where >1 population spike per stimulus occurred, was found in 10 of 45 (22%) slices from 20 Gdx rats and 0 of 56 slices in 24 sham rats (χ^2 test, $p<0.001$; Figure 6C). SD after TBS stimulation, occurred in 8 of 12 (75%) slices from 5 Gdx rats and 0 of 11 slices in 5 sham rats (Fisher's exact test, $p=0.001$; Figure 6C). Four of the 8 slices from Gdx rats that exhibited SD also showed more than one population spike/MF stimulus.

Another indication of abnormal excitability is shown in Figure 6D1. In this case, field potentials were repetitive but at a rhythm that was slower (~20 Hz) than the multiple population spikes in Figure 6A. CSD analysis (Figure 6D2–3) showed the stereotypical nature of the rhythmic field potentials across laminae of CA3 and that the earliest sink was in stratum lucidum (arrow in Figure 6D2–3), suggesting the MF pathway initiated activity. Five of 45 (11%) of slices from Gdx rats exhibited the rhythmic field potentials shown in Figure 6C–D; these were not the same slices that showed other signs of increased excitability in Figure 6A–B. Therefore, the total number of slices exhibiting hyperexcitability of one type or another was 19/45 or 42%.

The abnormal excitability that was recorded in Gdx rats was similar to the effects of recombinant BDNF superfused onto slices of normal adult male rats (Scharfman, 1997) and the responses to MF stimulation in rodents with elevated BDNF protein levels (Croll et al., 1999; Scharfman et al., 2003; Scharfman et al., 2007), which were blocked by the Trk receptor antagonist K252a (Scharfman, 1997; Scharfman et al., 2003; Scharfman et al., 2007). Therefore, we determined whether K252a would reduce excitability in Gdx rats.

As shown in Figure 7A, K252a reduced the first type of abnormal excitability in Gdx rats (>1 population spike/MF stimulus; Figure 6A). Specifically, perfusion of slices with 300 nM K252a for 15 min blocked the second population spike that was elicited by MF stimulation (n=3 slices, 2 rats; Figure 7A), and vehicle (0.003% DMSO) had no effect (2 slices from 2 other rats; data not shown). In slices where repetitive field potentials were elicited by a single stimulus (e.g., Figure 6D), an input-output curve for the amplitude of the first field potential was generated before and after exposure to K252a (Figure 7B1–3). There was a significant effect of K252a (two-way RMANOVA; $F(1,20)$ 87.483; $p<0.001$) and an interaction ($F(5,20)$ 15.129; $p<0.001$) with significant differences at all intensities above the minimum (where evoked potentials were negligible in all conditions; Student's t-tests, $p<0.05$; Figure 7B1–3). There was no effect of vehicle (pre vs. post vehicle, two-way RMANOVA; $F(5,20)$ 0.188; $p=0.687$; Figure 7B3).

To evaluate the effect of K252a on SD, SD was elicited by stimulus trains [(1 Hz, paired pulses for 10 sec, as described previously (Scharfman, 1997; Scharfman et al., 2003; Scharfman et al., 2007)] which were triggered once every 15 min (Figure 7C–D; K252a: n=3 slices, 3 Gdx rats; vehicle: n=3 slices, 3 other Gdx rats). After a 30 min baseline period, K252a was added to the ACSF for 15 min, followed by drug-free buffer (Figure 7C–D). There was a significant effect of K252a on the amplitude of SD episodes (measured from baseline to the peak of the SD episode; one-way RMANOVA; $F(9,29)$ 14.268; $p<0.001$) at 15 and 30 min after K252a was added (Paired t-test, $p=0.033$, 0.031 respectively; Figure 7D2). There were no detectable effects of vehicle (one-way RMANOVA; $F(9,29)$ 1.049; $p=0.442$; Figure 7D2). Taken together, the results suggested that a subset of Gdx rats exhibited hyperexcitability that was dependent on Trk receptors.

VI. BDNF protein expression increases in MFs after Gdx

Increased excitability in Gdx rats (Figures 6–7) was similar to rats or mice with elevation of BDNF levels in MFs (Croll et al., 1999; Scharfman et al., 2003; Scharfman et al., 2007). Therefore, we determined whether MF BDNF levels were increased in Gdx rats.

Initial experiments used a well-described polyclonal antibody to BDNF (Conner et al., 1997; Yan et al., 1997) and showed that Gdx rats (which had surgery at approximately 60 days of age and were evaluated approximately 2 weeks later) exhibited greater BDNF-ir in the MFs than sham rats (Figure 8A1–2).

Similar results were obtained using a second antibody (monoclonal; Figure 8B–D). Using the second antibody, 5 immunocytochemical procedures were conducted. For each procedure, a Gdx and sham littermate were subjected to surgery on the same day, at approximately 60 days of age (61.9 ± 2.0 days, n=5/group) followed by perfusion-fixation on the same day after surgery (12.0 ± 0.6 days) and brains were processed together. Sections from the 10 rats were quantified and analyzed in pairs (Gdx and sham). The location where the MF terminal plexus ends (Figure 9H1) was used for quantification because BDNF-ir was always greatest there, regardless of surgical pre-treatment (Figure 8D). The timeline of the experiments is shown in Figure 8E1 and the results, shown in Figure 8E2, demonstrated that MF BDNF-ir was greater in Gdx rats (Student's t-test, p=0.001).

A second experiment was conducted to determine if the increase in BDNF protein in MFs in Gdx rats was long-lasting (Figure 8F). For this purpose, rats were perfusion-fixed 2 months instead of 2 weeks after surgery (Figure 8F1). Again, surgery was conducted in pairs, so the age at surgery was the same (59.8 ± 1.0 days) and delays between surgery and perfusion were the same (61.2 ± 1.9 days, n=5/group). As shown in Figure 8F2, Gdx rats exhibited greater MF BDNF-ir than sham controls (Student's t-test, p=0.002). Therefore, the increase in MF BDNF-ir after Gdx appeared to be robust and long-lasting.

VII. Gdx rats exhibit MF sprouting

As recordings in stratum pyramidale and stratum oriens were conducted, it became clear that Gdx rats often exhibited fiber volleys and fEPSPs in these layers in response to MF stimulation (Figure 9A), leading to diverse sinks in these layers using CSD analysis (Figure 9B). These observations, and the results discussed above showing that BDNF-ir in MFs was elevated after Gdx, suggested that there was sprouting of MF axons into the pyramidal cell layer and stratum oriens of Gdx rats (diagrammed schematically in Figure 9A). Sprouting could be a response to increased BDNF levels in MFs, because BDNF application to the MFs has been suggested to induce MF axon outgrowth (Lowenstein and Arsenault, 1996; Tamura et al., 2006; Gomez-Palacio-Schjetnan and Escobar, 2008; Tamura et al., 2009), although all studies do not agree (Bender et al., 1998; Qiao et al., 2001; Shetty et al., 2003).

We determined if MF sprouting into stratum oriens occurred using dynorphin B as a marker of the MFs (Pierce et al., 1999). Immunocytochemical comparisons were made between Gdx and sham rats (n=7/group) that were perfused approximately 2 weeks after surgery (15.5 ± 2.7 days for each group). Animals were perfused and processed in pairs, with one Gdx and one sham rat subjected to surgery on the same day, perfused the same day, cut the same day, with identical delays between surgery and perfusion, and were processed at the same time (similar to the experiments discussed above for BDNF-ir). As shown in Figure 9C–F, Gdx rats exhibited a band of dynorphin-ir in stratum oriens of CA3a/b which was not evident in sham rats.

To quantify the differences in dynorphin-ir in Gdx rats compared to sham controls, a region of interest (ROI) was drawn around stratum lucidum, pyramidale and oriens to encompass

the area where dynorphin-ir was most robust in Gdx rats (Figure 9G1). Then the mean gray scale value was determined for that ROI, placing the same ROI over each section from each rat so that it covered stratum lucidum, stratum pyramidale and stratum oriens of CA3a/b (Figure 9G1). Next, the ROI was moved to stratum radiatum (Figure 9G1) where background staining was estimated, and subtracted from the first measurement. The results showed that the mean gray scale value for each Gdx rat was greater than the sham rat that was processed with it (Paired t-test, p=0.010; Figure 8G2).

An additional measurement was also made within the terminal plexus of the MF pathway in stratum lucidum near CA3 (Figure 9H1) to address the possibility that dynorphin-ir in the normal MF pathway increased after Gdx. As shown in Figure 9H2, there were no significant differences in dynorphin-ir (Student's t-test, p=0.487). Therefore, an increase in dynorphin expression in Gdx rats does not explain the increased dynorphin-ir in stratum oriens of Gdx rats in Figure 9C–G. Instead, the results suggest that new MFs developed in Gdx rats in stratum oriens.

Collectively the data suggest that Gdx rats exhibit MF sprouting approximately 2 weeks after surgery. There appeared to be a functional effect of the sprouted fibers because fEPSPs evoked by MF stimulation could be recorded throughout stratum lucidum, stratum pyramidale and stratum oriens of Gdx rats.

VIII. A Trk-dependent component of MF transmission and LTP emerges after Gdx

A. MF transmission in Gdx rats is reduced by K252a—Because the hyperexcitability in slices of Gdx rats was sensitive to K252a, and BDNF protein was increased in MFs, we asked if the increase in MF transmission and synaptic plasticity of Gdx rats would be K252a-sensitive. As shown in Figure 10A1, slices from Gdx and sham rats (n=4 slices from 4 rats/group) were recorded for a 15 min baseline period, exposed to vehicle (0.003% DMSO) and the responses that were recorded 30 min later were compared to the baseline. Next, slices were exposed to 300 nM K252a for 30 min, and subsequently slices were perfused with drug-free buffer for 30 min to determine if effects of K252a were reversible.

Drug effects were evaluated by two-way RMANOVA. There was a significant effect of surgical pre-treatment (Gdx or sham; $F(1,18)$ 28.092; p=0.002) and a significant interaction between the surgical pre-treatment and responses to drug treatments ($F(3,18)$ 6.995; p=0.003; Figure 10A2). The slope of fEPSPs in Gdx rats decreased in response to K252a (one-way RMANOVA; $F(3,15)$ 6.848; p=0.006; Student's t-test, p=0.013) to 61.0 ± 5.8% of control (Figure 10A2). There was no significant effect of K252a in sham controls (one-way RMANOVA; $F(3,15)$ 0.098; Student's t-test, p=0.965; Figure 10A2).

There was variable recovery after resuming drug-free buffer (Figure 10A2; wash, white circle with large standard error of the mean), unlike shorter periods of K252a application in previous experiments where recovery was more consistent (Figure 7; similar standard error bars during the experiments). These data suggested that prolonged exposure to dilute DMSO, first as the vehicle pre-treatment and then as the K252a solvent, had adverse effects, leading to inability of some slices to recover during wash. Therefore we also evaluated K252a in slices without pretreatment with dilute DMSO (n=8 slices, 8 Gdx rats; Figure 10B1). As shown in Figure 10B2, K252a depressed the fEPSP slope and there was more consistent recovery. Taken together, these data suggest that a Trk-sensitive component of MF transmission emerged after Gdx that was not normally present in sham rats.

B. MF LTP in Gdx rats is reduced by K252a—To test the effect of K252a on LTP, a 15-min long baseline was followed by exposure to 300 nM K252a for 15 min, the latency

when K252a began to exert an effect in Figure 10B. After LTP induction, K252a exposure continued for another 15 min, followed by perfusion with drug-free buffer (Figure 10C). For comparison, slices were exposed to vehicle for 15 min before and after LTP induction (Figure 10C).

K252a-treated slices had less LTP than vehicle-treated slices: 60 minutes after LTP induction, fEPSP slopes in K252a-treated slices were 62.8 ± 17.1% of control (n=6 slices, 6 Gdx rats; Figure 10C) whereas vehicle-treated slices exhibited 113.7 ± 12.7% potentiation (n=7 slices, 7 Gdx rats) which weres significantly different (Student's t-test; p=0.031). K252a-treated slices of Gdx rats were not significantly different from slices of sham rats that were untreated (Student's t-test, p=0.439), suggesting that K252a reversed the effect of Gdx (Figure 10C).

K252a-treated slices from Gdx rats also showed decreased PTP relative to vehicle-treated slices; two-way RMANOVA showed that there was an interaction between treatment (K252a vs. vehicle) and PTP (F (9,99) 2.441; p=0.015) with K252a-treated slices showing significantly decreased PTP immediately after LTP induction (Student's t-test, p=0.006) and at 2 min (p=0.017), but not other times.

These data were consistent with the hypothesis that a Trk-sensitive component of synaptic plasticity emerged after Gdx. However, LTP in vehicle-treated slices was reduced compared to untreated slices of Gdx rats (p=0.036; Figure 10C), suggesting an adverse effect of vehicle. An effect of vehicle was also suspected based on data in Figure 10A2 where there was inconsistent recovery after prolonged application of vehicle (exposure to vehicle alone, then K252a dissolved in vehicle). Therefore, we also tested the effect of a scavenger of BDNF, TrkB-IgG, where vehicle was 0.9% NaCl. TrkB-IgG protein is a composed of the recognition site of TrkB and the FC region of human IgG1 (Binder et al., 1999). Comparison was to human IgG1. The concentration of TrkB was chosen because of its efficacy in previous studies (Kang et al., 1996; Skucas et al., 2011).

As shown in Figure 10D, TrkB-IgG suppressed LTP compared to IgG. TrkB-IgG-treated slices exhibited 112.4 ± 12.0% potentiation at 60 min following LTP induction (n=7 slices, 6 Gdx rats), compared to 141.7 ± 6.9% potentiation in IgG-treated slices (n=9 slices, 6 Gdx rats; Student's t-test, p=0.030). LTP in IgG-treated slices of Gdx rats was not significantly different from untreated slices of Gdx rats (Student's t-test, p=0.674). PTP was reduced by TrkB-IgG compared to IgG: 1 min after LTP induction, PTP was 191.4 ± 15.7% in TrkB-IgG treated slices and 251.7 ± 21.6% in IgG-treated slices (Student's t-test, p=0.036).

Taken together, these data suggest that a Trk-sensitive component of MF PTP and LTP emerged after Gdx.

DISCUSSION

The results show that MF transmission, excitability and plasticity in area CA3 increase after Gdx in adult male rats. The mechanisms involve an increase in androgen receptor-dependent and Trk-dependent signaling. The results are relevant to sex differences in hippocampus, and clarifying the role of androgens in hippocampal function. With a few exceptions (Mizoguchi et al., 1992; Isgor and Sengelaub, 2003; Kaminski et al., 2005; Hatanaka et al., 2009), information about the effects of androgens in area CA3 is particularly limited. The results are also relevant to conditions when circulating androgens are decreased, such as aging (Gooren, 2003; Yeap, 2009), and disorders where androgens have been implicated in the underlying pathophysiology (Herzog, 1991; Harden and MacLusky, 2004; Harden and MacLusky, 2005; Frye, 2006; Becker et al., 2008; Drummond et al., 2009; Etgen and Pfaff, 2009; Al Sweidi et al., 2011; Barron and Pike, 2011).

Alterations in area CA3 after Gdx

The results show that diverse effects of Gdx occur in area CA3, including 1) an increase in MF transmission, PPF, and LTP, 2) the emergence of a DHT-sensitive component of MF transmission and LTP, and 3) increased MF BDNF expression, MF sprouting, and Trk-dependent increases in MF transmission and excitability.

1) MF transmission, PPF and LTP—MF transmission increased in Gdx rats because there was an increase in MF fEPSP slope and amplitude. There was an increase in fiber volley amplitude without a change in latency, suggesting an increase in axonal excitability but no change in the timing of synaptic transmission. In addition, population spike amplitude was increased in slices from Gdx rats, suggesting increased CA3 pyramidal cell output. Consistent with this finding, recurrent fEPSPs elicited by MF stimulation were increased. PPF was increased in Gdx rats, suggesting that short-term plasticity was enhanced. Short interstimulus intervals (10–20 msec) were unaffected, suggesting that feedback inhibition was unchanged. A neurosteroid acting on $GABA_A$ receptors (Adiol) did not reverse effects of Gdx, suggesting that disinhibition, at least at the 2 week timepoint after Gdx, did not cause the effects of Gdx in slices. However, the possible effects of acute depletion of Adiol in the first days after Gdx, and a comprehensive study of GABAergic inhibition 2 weeks after Gdx, is necessary before ruling out a role of reduced GABAergic inhibition.. It is important to note that PPF was low in the control animals (relative to younger rodents; e.g., Salin et al., 1996), which we think is because of the older ages (>60 days old) in the present study; under our recordings conditions there is greater PPF if younger rats (~30 days) are used (unpublished data).

Using a stimulus paradigm that induces LTP in young rats [18–25 days; (Kwon and Castillo, 2008)], Gdx rats exhibited robust LTP. This result suggests that long-term synaptic plasticity of the MFs was altered by Gdx. If this result can be generalized to behavior, one would predict a greater ability of the CA3 network to exhibit behavioral plasticity in Gdx rats. For example, Gdx rats might exhibit better pattern separation and completion, where the MF pathway has been suggested to play a pivotal role (Derrick, 2007; Jaffe and Gutierrez, 2007). However, Gdx rats showed a reduction in the specificity of MFs for stratum lucidum. Therefore, area CA3 of Gdx rats could exhibit a gain of function due to increased synaptic plasticity or a loss of function because of reduced MF specificity. Indeed, Gdx rats show both impaired and improved hippocampal function in behavioral tests (Edinger and Frye, 2004; Edinger et al., 2004; Edinger and Frye, 2007a; Frye et al., 2008; Harooni et al., 2008).

It is noteable that the Gdx rats exhibited LTP but sham controls did not. This difference could reflect greater plasticity in Gdx rats, but it also can be interpreted as a change in threshold for LTP induction. Thus, the stimulus parameters (frequency, synaptic strength) used to elicit LTP in Gdx rats may be distinct from sham controls.

2) DHT-sensitivity of MF transmission and LTP after Gdx—DHT exerted robust effects in slices of Gdx rats, normalizing MF fEPSPs and MF LTP as late as 2–3 weeks after Gdx. It is remarkable that brief exposure to DHT could normalize MF transmission given that changes in BDNF synthesis and axonal sprouting take more time. The results raise the possibility that Gdx makes the MF pathway sensitive to acute androgen exposure when it normally is not. One mechanism is that androgen receptors on the cell surface are normally downregulated in the presence of normal testosterone levels. Therefore, addition of more androgen *in vitro* cannot elicit a detectable effect. This explanation has experimental support: cell surface expression of androgen receptors increases in response to reduced levels of circulating androgens (Kerr et al., 1995; Fargo et al., 2009; Meyer et al., 2009;

Hsieh et al., 2011). Alternatively, increased androgen receptor expression at the cell surface of Gdx rats could be a compensatory response to increased excitability.

One can not rule out the possibility that other metabolites of testosterone besides DHT contributed to the effects of Gdx. Regarding the metabolite of DHT that acts on $GABA_A$ receptors, Adiol (5α-androstane-3α, 17β-diol), there were no detectable effects under conditions in which DHT exerted a robust influence. However, it is possible that Adiol would have exhibited effects if examined in other experimental paradigms. Regarding metabolites of testosterone that act on estrogen receptors [(17β-estradiol and 5α-androstane-3β, 17β-diol (Pak et al., 2004; Handa et al., 2008; Handa et al. 2011)], one cannot rule out effects of these metabolites either. Although some studies suggest that males are relatively insensitive to 17β-estradiol compared to females, for example in the number of hippocampal CA1 spine synapses that increase in response to 17β-estradiol administration (Maclusky et al., 2006; Woolley and McEwen, 1992; Cooke and Woolley, 2005; Woolley, 2007), and other measures of hippocampal function (Huang and Woolley, 2012; Vierk et al., 2012), other studies have shown robust effects of 17β-estradiol in males (Foy et al., 1999; Mukai et al., 2006; Murakami et al., 2006; Kramar et al., 2009; Mukai et al., 2009; Grassi et al., 2011; Kramar et al., 2012).

It is surprising that acute exposure to Adiol (5α-androstane-3α, 17β-diol) had no effect in slices from sham or Gdx rats because others have found effects, and these are consistent with enhanced GABAergic inhibition, such as inhibition of convulsant-induced seizures *in vivo* or reduction in epileptiform discharges *in vitro* (Reddy, 2004a; b). One possible explanation is that Adiol has more robust effects on seizure activity than normal activity. It is also possible that the high concentrations of Adiol cause direct (agonist) actions at the $GABA_A$ receptor (Penatti and Henderson, 2009; Reddy, 2010). High concentrations of Adiol may also be effective because Adiol can be converted to DHT.

3) Increased BDNF expression, Trk-dependence of MF transmission and excitability, and MF sprouting after Gdx—The results are consistent with previous studies in males showing that K252a blocks hyperexcitability induced by exposure of hippocampal slices to BDNF (Scharfman, 1997), and are consistent with excitatory effects of BDNF in males that have been observed *in vivo* (Gomez-Palacio-Schjetnan and Escobar, 2008; Schjetnan and Escobar, 2010), as well as other subfields [area CA1: (Lu et al., 2008; Minichiello, 2009); dentate gyrus: (Bramham, 2007)]. In addition, the results are consistent with studies showing that K252a blocked hyperexcitability evoked by MF stimuli in male C57bl6 mice when BDNF was constitutively overexpressed (Croll et al., 1999), and female rats where MF BDNF was elevated (Scharfman et al., 2003; Scharfman et al., 2007).

The mechanism by which androgen depletion regulates MF BDNF synthesis could be similar to the mechanism proposed for 17β-estradiol: a direct effect on a putative estrogen response element in the BDNF gene (Sohrabji et al., 1995). Androgen response elements exist (Fargo et al., 2009), but it is not clear if androgen response elements are present on the BDNF gene. Another potential mechanism is activity-dependent synthesis of BDNF (Isackson et al., 1991; Aid et al., 2007) which has been suggested (Blurton-Jones and Tuszynski, 2006). Because Gdx increases neuronal excitability, it could induce MF BDNF expression by this mechanism.

It is noteworthy that 17β-estradiol exerts its effects on synaptic plasticity in area CA1 by regulating the cytoskeleton (Kramar et al., 2012). A similar mechanism could be responsible for effects of Gdx (e.g., sprouting), especially in light of the evidence that local estradiol synthesis occurs in the male and exert effects (Grassi et al., 2011).

Gdx effects on the MF pathway: a presynaptic site of action?

Increased PPF and PTP in Gdx rats support a presynaptic site of action. This idea is consistent with the evidence that androgen receptors and Trk receptors are present in MF terminals (Tabori et al., 2005). A presynaptic mechanism also could explain increased MF LTP in Gdx rats because an LTP induction protocol was used that is similar to one that induces LTP by a presynaptic mechanism (Kwon and Castillo, 2008). MF sprouting and increased BDNF in MFs of Gdx rats could also contribute to a change in MF transmission that is presynaptic. Notably, BDNF increases transmitter release at other hippocampal synapses (Xu et al., 2000; Tyler et al., 2006) and in prior studies of normal adult males, BDNF appeared to act on presynaptic Trk receptors to increase MF transmission (Scharfman, 1997). However, the dendritic targeting of BDNF (Tongiorgi, 2008) which can trigger critical events in LTP (Bramham, 2007), suggests postsynaptic sites are also important to consider.

Implications

The data presented here suggest that the effects of androgens in hippocampus are more complex than previously considered. The impression created by past studies is that gonadal steroids confer hippocampal plasticity, and the response to Gdx in males and females is at least superficially similar (MacLusky et al., 2006). The data presented here suggest that this is not the case. While ovariectomy of female rats decreases MF BDNF expression and area CA3 excitability, 17β-estradiol restores it (Scharfman et al., 2003; Scharfman et al., 2007). Gdx of male rats has the opposite effect, increasing BDNF levels and excitability.

The results suggest potential mechanisms for the clinical findings that have been reported in patients with androgen deprivation or androgen excess. It has been suggested that low serum androgen levels increase the risk for diseases which involve the hippocampus such as temporal lobe epilepsy (Herzog, 1991; Harden and MacLusky, 2004; Harden and MacLusky, 2005), at least in part because of the loss of Adiol and consequent reduction in GABAergic inhibition (Frye, 2006; Reddy and Jian, 2010). The results of the present study suggest an additional mechanism: loss of androgen increases excitability by androgen receptor- and Trk-dependent mechanisms. The decrease in CA1spine synapss in males following Gdx, previously reported (MacLusky et al., 2006), may be counterbalanced by rising BDNF, increasing MF transmission, excitability and plasticity. Even if the increase in CA3 excitability is restricted to the initial weeks following androgen depletion, as was studied here, it appears to initiate long lasting effects on BDNF synthesis and MF sprouting, and could therefore contribute to the increased incidence of epilepsy with age (Hauser and Hesdorffer, 1990).

The data are also relevant to androgen ablation therapy. The results of the present study suggest a possible explanation for the observation that adverse cognitive effects do not necessarily occur during therapy (Nelson et al., 2008; Alibhai et al., 2010a; Alibhai et al., 2010b). Function may be partially preserved because of an increase in synaptic transmission and plasticity mediated by BDNF in CA3.

Our results also shed suggest mechanisms for the adverse effects of androgen abuse in men. Psychiatric disturbances such as mood disorders or aggressive behavior are a common adverse effect in males abusing anabolic androgenic steroids (Pope and Katz, 1994). Because low hippocampal BDNF levels are common in depression (Shimizu et al., 2003; Wang et al., 2008), it is possible that high levels of anabolic androgens could exert adverse effects on mood by suppressing hippocampal BDNF expression. Indeed, anabolic androgenic steroids lower BDNF levels in hippocampus and prefrontal cortex of rats, leading to a depressed phenotype (Matrisciano et al., 2012). A similar mechanism could

underly aggressive behavior after abuse of anabolic androgens based on mice with a conditional BDNF deletion (interestingly, it was primarily in the dentate gyrus and area CA3) which show increased aggression (Ito et al., 2011). Furthermore, mice bred for increased aggression have a smaller MF plexus in stratum oriens (Sluyter et al., 1994). Therefore, it is possible that high levels of androgens suppress MF BDNF and reduce the MF plexus, contributing to both depression and aggressive behavior.

Acknowledgments

This study was supported by R01 NS 37562 and T32 MH 097763. We thank Teresa A. Milner for the antibody to dynorphin and Joseph P. Pierce for discussion.

References

Aid T, Kazantseva A, Piirsoo M, Palm K, Timmusk T. Mouse and rat BDNF gene structure and expression revisited. J Neurosci Res. 2007; 85:525–535. [PubMed: 17149751]

Al Sweidi S, Sanchez MG, Bourque M, Morissette M, Dluzen D, Di Paolo T. Oestrogen receptors and signalling pathways: Implications for neuroprotective effects of sex steroids in Parkinson's disease. J Neuroendocrinol. 2011; 24:48–61. [PubMed: 21790809]

Alibhai SM, Breunis H, Timilshina N, Marzouk S, Stewart D, Tannock I, Naglie G, Tomlinson G, Fleshner N, Krahn M, Warde P, Canning SD. Impact of androgen-deprivation therapy on cognitive function in men with nonmetastatic prostate cancer. J Clin Oncol. 2010a; 28:5030–5037. [PubMed: 21041708]

Alibhai SM, Mahmoud S, Hussain F, Naglie G, Tannock I, Tomlinson G, Fleshner N, Krahn M, Warde P, Klotz L, Breunis H, Leach M, Canning SD. Levels of sex hormones have limited effect on cognition in older men with or without prostate cancer. Crit Rev Oncol Hematol. 2010b; 73:167–175. [PubMed: 19346137]

Almeida OP, Flicker L. Testosterone and dementia: Too much ado about too little data. J Br Menopause Soc. 2003; 9:107–110. [PubMed: 14670195]

Barha CK, Galea LA. Influence of different estrogens on neuroplasticity and cognition in the hippocampus. Biochim Biophys Acta. 2010; 1800:1056–1067. [PubMed: 20100545]

Barron AM, Pike CJ. Sex hormones, aging, and Alzheimer's disease. Front Biosci (Elite Ed). 2011; 4:976–997. [PubMed: 22201929]

Becker, JB.; Berkely, KJ.; Geary, I.; Hampson, E.; Herman, JP.; Young, E., editors. Sex differences in the brain: From genes to behavior. Oxford: Oxford University Press; 2008.

Bender R, Heimrich B, Meyer M, Frotscher M. Hippocampal mossy fiber sprouting is not impaired in brain-derived neurotrophic factor-deficient mice. Exp Brain Res. 1998; 120:399–402. [PubMed: 9628426]

Binder DK, Routbort MJ, Ryan TE, Yancopoulos GD, McNamara JO. Selective inhibition of kindling development by intraventricular administration of trkb receptor body. J Neurosci. 1999; 19:1424–1436. [PubMed: 9952419]

Blurton-Jones M, Tuszynski MH. Estradiol-induced modulation of estrogen receptor-beta and GABA within the adult neocortex: A potential transsynaptic mechanism for estrogen modulation of BDNF. J Comp Neurol. 2006; 499:603–612. [PubMed: 17029253]

Bramham CR. Control of synaptic consolidation in the dentate gyrus: Mechanisms, functions, and therapeutic implications. Prog Brain Res. 2007; 163:453–471. [PubMed: 17765733]

Brown TJ, Sharma M, MacLusky NJ. Localization and measurement of occupied androgen receptors in thaw-mounted rat and human prostate tissue sections by in vitro autoradiography. Steroids. 1995; 60:239–247. [PubMed: 7618192]

Chakraborty G, Magagna-Poveda A, Parratt C, Umans JG, MacLusky NJ, Scharfman HE. Reduced hippocampal brain-derived neurotrophic factor (BDNF) in neonatal rats after prenatal exposure to propylthiouracil (PTU). Endocrinology. 2012; 153:1311–1316. [PubMed: 22253429]

Cherrier MM, Matsumoto AM, Amory JK, Asthana S, Bremner W, Peskind ER, Raskind MA, Craft S. Testosterone improves spatial memory in men with Alzheimer disease and mild cognitive impairment. Neurology. 2005; 64:2063–2068. [PubMed: 15985573]

Chetyrkin SV, Hu J, Gough WH, Dumaual N, Kedishvili NY. Further characterization of human microsomal 3α-hydroxysteroid dehydrogenase. Arch Biochem Biophys. 2001; 386:1–10. [PubMed: 11360992]

Claiborne BJ, Xiang Z, Brown TH. Hippocampal circuitry complicates analysis of long-term potentiation in mossy fiber synapses. Hippocampus. 1993; 3:115–121. [PubMed: 8353597]

Clancy AN, Bonsall RW, Michael RP. Immunohistochemical labeling of androgen receptors in the brain of rat and monkey. Life Sci. 1992; 50:409–417. [PubMed: 1734159]

Conner JM, Lauterborn JC, Yan Q, Gall CM, Varon S. Distribution of brain-derived neurotrophic factor (BDNF) protein and mRNA in the normal adult rat CNS: Evidence for anterograde axonal transport. J Neurosci. 1997; 17:2295–2313. [PubMed: 9065491]

Cosgrove KE, Galvan EJ, Meriney SD, Barrionuevo G. Area CA3 interneurons receive two spatially segregated mossy fiber inputs. Hippocampus. 2009; 20:1003–1009. [PubMed: 19830814]

Croll SD, Suri C, Compton DL, Simmons MV, Yancopoulos GD, Lindsay RM, Wiegand SJ, Rudge JS, Scharfman HE. Brain-derived neurotrophic factor transgenic mice exhibit passive avoidance deficits, increased seizure severity and in vitro hyperexcitability in the hippocampus and entorhinal cortex. Neuroscience. 1999; 93:1491–1506. [PubMed: 10501474]

Derrick BE. Plastic processes in the dentate gyrus: A computational perspective. Prog Brain Res. 2007; 163:417–451. [PubMed: 17765732]

DonCarlos LL, Garcia-Ovejero D, Sarkey S, Garcia-Segura LM, Azcoitia I. Androgen receptor immunoreactivity in forebrain axons and dendrites in the rat. Endocrinology. 2003; 144:3632–3638. [PubMed: 12865346]

Driscoll I, Resnick SM. Testosterone and cognition in normal aging and Alzheimer's disease: An update. Curr Alzheimer Res. 2007; 4:33–45. [PubMed: 17316164]

Drummond ES, Harvey AR, Martins RN. Androgens and Alzheimer's disease. Curr Opin Endocrinol Diabetes Obes. 2009; 16:254–259. [PubMed: 19373081]

Edinger KL, Frye CA. Testosterone's analgesic, anxiolytic, and cognitive-enhancing effects may be due in part to actions of its 5α-reduced metabolites in the hippocampus. Behav Neurosci. 2004; 118:1352–1364. [PubMed: 15598144]

Edinger KL, Frye CA. Testosterone's anti-anxiety and analgesic effects may be due in part to actions of its 5α-reduced metabolites in the hippocampus. Psychoneuroendocrinology. 2005; 30:418–430. [PubMed: 15721054]

Edinger KL, Frye CA. Androgens' effects to enhance learning may be mediated in part through actions at estrogen receptor-β in the hippocampus. Neurobiol Learn Mem. 2007a; 87:78–85. [PubMed: 16904920]

Edinger KL, Frye CA. Androgens' performance-enhancing effects in the inhibitory avoidance and water maze tasks may involve actions at intracellular androgen receptors in the dorsal hippocampus. Neurobiol Learn Mem. 2007b; 87:201–208. [PubMed: 17029870]

Edinger KL, Lee B, Frye CA. Mnemonic effects of testosterone and its 5α-reduced metabolites in the conditioned fear and inhibitory avoidance tasks. Pharmacol Biochem Behav. 2004; 78:559–568. [PubMed: 15251265]

Edwards HE, Burnham WM, MacLusky NJ. Testosterone and its metabolites affect afterdischarge thresholds and the development of amygdala kindled seizures. Brain Res. 1999; 838:151–157. [PubMed: 10446327]

Etgen, AM.; Pfaff, D., editors. Molecular mechanisms of hormone action. New York: Academic Press; 2009.

Fargo, KN.; Pak, TR.; Foecking, EM.; Jones, KJ. Molecular biology of androgen action. In: Etgen, A.; Pfaff, D., editors. Molecular mechanisms of hormone action on behavior. New York: Academic Press; 2009.

Fester L, Prange-Kiel J, Zhou L, Blittersdorf BV, Bohm J, Jarry H, Schumacher M, Rune GM. Estrogen-regulated synaptogenesis in the hippocampus: Sexual dimorphism in vivo but not in vitro. J Steroid Biochem Mol Biol. 2011; 131:24–29. [PubMed: 22138012]

Foy MR. Ovarian hormones, aging and stress on hippocampal synaptic plasticity. Neurobiol Learn Mem. 2010; 95:134–144. [PubMed: 21081173]

Foy MR, Xu J, Xie X, Brinton RD, Thompson RF, Berger TW. 17β-estradiol enhances NMDA receptor-mediated EPSPs and long-term potentiation. J Neurophysiol. 1999; 81:925–929. [PubMed: 10036289]

Frye CA. Role of androgens in epilepsy. Expert Rev Neurother. 2006; 6:1061–1075. [PubMed: 16831119]

Frye CA, Edinger KL. Testosterone's metabolism in the hippocampus may mediate its anti-anxiety effects in male rats. Pharmacol Biochem Behav. 2004; 78:473–481. [PubMed: 15251256]

Frye CA, Edinger K, Sumida K. Androgen administration to aged male mice increases anti-anxiety behavior and enhances cognitive performance. Neuropsychopharmacology. 2008; 33:1049–1061. [PubMed: 17625503]

Frye CA, Edinger KL, Seliga AM, Wawrzycki JM. 5α-reduced androgens may have actions in the hippocampus to enhance cognitive performance of male rats. Psychoneuroendocrinology. 2004; 29:1019–1027. [PubMed: 15219653]

Frye CA, Edinger KL, Lephart ED, Walf AA. 3α-androstanediol, but not testosterone, attenuates age-related decrements in cognitive, anxiety, and depressive behavior of male rats. Front Aging Neurosci. 2010; 2:15. [PubMed: 20552051]

Frye CA, Park D, Tanaka M, Rosellini R, Svare B. The testosterone metabolite and neurosteroid 3α-androstanediol may mediate the effects of testosterone on conditioned place preference. Psychoneuroendocrinology. 2001; 26:731–750. [PubMed: 11500254]

Fuller SJ, Tan RS, Martins RN. Androgens in the etiology of Alzheimer's disease in aging men and possible therapeutic interventions. J Alzheimers Dis. 2007; 12:129–142. [PubMed: 17917157]

Galea LA. Gonadal hormone modulation of neurogenesis in the dentate gyrus of adult male and female rodents. Brain Res Rev. 2008; 57:332–341. [PubMed: 17669502]

Gomez-Palacio-Schjetnan A, Escobar ML. In vivo BDNF modulation of adult functional and morphological synaptic plasticity at hippocampal mossy fibers. Neurosci Lett. 2008; 445:62–67. [PubMed: 18782600]

Gooren L. Testosterone supplementation: Why and for whom? Aging Male. 2003; 6:184–199. [PubMed: 14628499]

Grassi S, Tozzi A, Costa C, Tantucci M, Colcelli E, Scarduzio M, Calabresi P, Pettorossi VE. Neural 17β-estradiol facilitates long-term potentiation in the hippocampal CA1 region. Neuroscience. 2011; 192:67–73. [PubMed: 21749911]

Handa RJ, Ogawa S, Wang JM, Herbison AE. Roles for oestrogen receptor β in adult brain function. J Neuroendocrinol. 2011; 24:160–173. [PubMed: 21851428]

Handa RJ, Pak TR, Kudwa AE, Lund TD, Hinds L. An alternate pathway for androgen regulation of brain function: Activation of estrogen receptor β by the metabolite of dihydrotestosterone, 5α-androstane-3β,17β-diol. Horm Behav. 2008; 53:741–752. [PubMed: 18067894]

Harden C, MacLusky NJ. Aromatase inhibition, testosterone, and seizures. Epilepsy Behav. 2004; 5:260–263. [PubMed: 15123030]

Harden C, MacLusky NJ. Aromatase inhibitors as add-on treatment for men with epilepsy. Expert Rev Neurother. 2005; 5:123–127. [PubMed: 15853482]

Harley CW, Malsbury CW, Squires A, Brown RA. Testosterone decreases CA1 plasticity in vivo in gonadectomized male rats. Hippocampus. 2000; 10:693–697. [PubMed: 11153715]

Harooni HE, Naghdi N, Sepehri H, Rohani AH. Intra hippocampal injection of testosterone impaired acquisition, consolidation and retrieval of inhibitory avoidance learning and memory in adult male rats. Behav Brain Res. 2008; 188:71–77. [PubMed: 18054400]

Hatanaka Y, Mukai H, Mitsuhashi K, Hojo Y, Murakami G, Komatsuzaki Y, Sato R, Kawato S. Androgen rapidly increases dendritic thorns of CA3 neurons in male rat hippocampus. Biochem Biophys Res Commun. 2009; 381:728–732. [PubMed: 19254689]

Hauser, WA.; Hesdorffer, DC. Epilepsy: frequency, causes and consequences. Landover, MD: Epilepsy Foundation of America; 1990.

Herzog AG. Reproductive endocrine considerations and hormonal therapy for men with epilepsy. Epilepsia. 1991; 32(Suppl 6):S34–37. [PubMed: 1959510]

Hsieh JT, Chen SC, Yu HJ, Chang HC. Finasteride upregulates expression of androgen receptor in hyperplastic prostate and lncap cells: Implications for chemoprevention of prostate cancer. Prostate. 2011; 71:1115–1121. [PubMed: 21557276]

Huang GZ, Woolley CS. Estradiol acutely suppresses inhibition in the hippocampus through a sex-specific endocannabinoid and mglur-dependent mechanism. Neuron. 2012; 74:801–808. [PubMed: 22681685]

Isackson PJ, Huntsman MM, Murray KD, Gall CM. BDNF mRNA expression is increased in adult rat forebrain after limbic seizures: Temporal patterns of induction distinct from NGF. Neuron. 1991; 6:937–948. [PubMed: 2054188]

Isgor C, Sengelaub DR. Effects of neonatal gonadal steroids on adult CA3 pyramidal neuron dendritic morphology and spatial memory in rats. J Neurobiol. 2003; 55:179–190. [PubMed: 12672016]

Ito W, Chehab M, Thakur S, Li J, Morozov A. BDNF-restricted knockout mice as an animal model for aggression. Genes Brain Behav. 2011; 10:365–374. [PubMed: 21255268]

Jaffe DB, Gutierrez R. Mossy fiber synaptic transmission: Communication from the dentate gyrus to area CA3. Prog Brain Res. 2007; 163:109–132. [PubMed: 17765714]

Kaminski RM, Marini H, Kim WJ, Rogawski MA. Anticonvulsant activity of androsterone and etiocholanolone. Epilepsia. 2005; 46:819–827. [PubMed: 15946323]

Kamiya H, Ozawa S, Manabe T. Kainate receptor-dependent short-term plasticity of presynaptic ca2+ influx at the hippocampal mossy fiber synapses. J Neurosci. 2002; 22:9237–9243. [PubMed: 12417649]

Kang H, Jia LZ, Suh KY, Tang L, Schuman EM. Determinants of BDNF-induced hippocampal synaptic plasticity: Role of the trk b receptor and the kinetics of neurotrophin delivery. Learn Mem. 1996; 3:188–196. [PubMed: 10456089]

Kerr JE, Allore RJ, Beck SG, Handa RJ. Distribution and hormonal regulation of androgen receptor (AR) and AR messenger ribonucleic acid in the rat hippocampus. Endocrinology. 1995; 136:3213–3221. [PubMed: 7628354]

Kramar EA, Babayan AH, Gall CM, Lynch G. Estrogen promotes learning-related plasticity by modifying the synaptic cytoskeleton. Neuroscience. 2012 in press.

Kramar EA, Chen LY, Brandon NJ, Rex CS, Liu F, Gall CM, Lynch G. Cytoskeletal changes underlie estrogen's acute effects on synaptic transmission and plasticity. J Neurosci. 2009; 29:12982–12993. [PubMed: 19828812]

Kwon HB, Castillo PE. Long-term potentiation selectively expressed by NMDA receptors at hippocampal mossy fiber synapses. Neuron. 2008; 57:108–120. [PubMed: 18184568]

Leranth C, Petnehazy O, MacLusky NJ. Gonadal hormones affect spine synaptic density in the CA1 hippocampal subfield of male rats. J Neurosci. 2003; 23:1588–1592. [PubMed: 12629162]

Lorente de No R. Studies on the structure of the cerebral cortex. Continuation of the study of the ammonic system. J Psychol Neurol. 1934; 46:113–177.

Lowenstein DH, Arsenault L. Dentate granule cell layer collagen explant cultures: Spontaneous axonal growth and induction by brain-derived neurotrophic factor or basic fibroblast growth factor. Neuroscience. 1996; 74:1197–1208. [PubMed: 8895886]

Lu Y, Christian K, Lu B. BDNF: A key regulator for protein synthesis-dependent LTP and long-term memory? Neurobiol Learn Mem. 2008; 89:312–323. [PubMed: 17942328]

Luchetti S, Huitinga I, Swaab DF. Neurosteroid and $GABA_A$ receptor alterations in Alzheimer's disease, Parkinson's disease and multiple sclerosis. Neuroscience. 2011; 191:6–21. [PubMed: 21514366]

MacLusky NJ, Hajszan T, Prange-Kiel J, Leranth C. Androgen modulation of hippocampal synaptic plasticity. Neuroscience. 2006; 138:957–965. [PubMed: 16488544]

Matousek RH, Sherwin BB. Sex steroid hormones and cognitive functioning in healthy, older men. Horm Behav. 2010; 57:352–359. [PubMed: 20079740]

Matrisciano F, Modafferi AM, Togna GI, Barone Y, Pinna G, Nicoletti F, Scaccianoce S. Repeated anabolic androgenic steroid treatment causes antidepressant-reversible alterations of the hypothalamic-pituitary-adrenal axis, BDNF levels and behavior. Neuropharmacology. 2012; 58:1078–1084. [PubMed: 20138062]

McEwen BS, Milner TA. Hippocampal formation: Shedding light on the influence of sex and stress on the brain. Brain Res Rev. 2007; 55:343–355. [PubMed: 17395265]

McLaughlin KJ, Baran SE, Conrad CD. Chronic stress- and sex-specific neuromorphological and functional changes in limbic structures. Mol Neurobiol. 2009; 40:166–182. [PubMed: 19653136]

Meyer RP, Gehlhaus M, Schwab R, Burck C, Knoth R, Hagemeyer CE. Concordant up-regulation of cytochrome P450 Cyp3a11, testosterone oxidation and androgen receptor expression in mouse brain after xenobiotic treatment. J Neurochem. 2009; 109:670–681. [PubMed: 19226368]

Minichiello L. Trkb signalling pathways in ltp and learning. Nat Rev Neurosci. 2009; 10:850–860. [PubMed: 19927149]

Mitsushima D. Sex differences in the septo-hippocampal cholinergic system in rats: Behavioral consequences. Curr Top Behav Neurosci. 2011; 8:57–71. [PubMed: 21769723]

Mitsushima D, Takase K, Takahashi T, Kimura F. Activational and organisational effects of gonadal steroids on sex-specific acetylcholine release in the dorsal hippocampus. J Neuroendocrinol. 2009; 21:400–405. [PubMed: 19356199]

Mizoguchi K, Kunishita T, Chui DH, Tabira T. Stress induces neuronal death in the hippocampus of castrated rats. Neurosci Lett. 1992; 138:157–160. [PubMed: 1407656]

Mukai H, Tsurugizawa T, Ogiue-Ikeda M, Murakami G, Hojo Y, Ishii H, Kimoto T, Kawato S. Local neurosteroid production in the hippocampus: Influence on synaptic plasticity of memory. Neuroendocrinology. 2006; 84:255–263. [PubMed: 17142999]

Mukai H, Kimoto T, Hojo Y, Kawato S, Murakami G, Higo S, Hatanaka Y, Ogiue-Ikeda M. Modulation of synaptic plasticity by brain estrogen in the hippocampus. Biochim Biophys Acta. 2009; 1800:1030–1044. [PubMed: 19909788]

Murakami G, Tsurugizawa T, Hatanaka Y, Komatsuzaki Y, Tanabe N, Mukai H, Hojo Y, Kominami S, Yamazaki T, Kimoto T, Kawato S. Comparison between basal and apical dendritic spines in estrogen-induced rapid spinogenesis of CA1 principal neurons in the adult hippocampus. Biochem Biophys Res Commun. 2006; 351:553–558. [PubMed: 17070772]

Naghdi N, Asadollahi A. Genomic and nongenomic effects of intrahippocampal microinjection of testosterone on long-term memory in male adult rats. Behav Brain Res. 2004; 153:1–6. [PubMed: 15219700]

Naghdi N, Majlessi N, Bozorgmehr T. The effect of intrahippocampal injection of testosterone enanthate (an androgen receptor agonist) and anisomycin (protein synthesis inhibitor) on spatial learning and memory in adult, male rats. Behav Brain Res. 2005; 156:263–268. [PubMed: 15582112]

Nelson CJ, Lee JS, Gamboa MC, Roth AJ. Cognitive effects of hormone therapy in men with prostate cancer: A review. Cancer. 2008; 113:1097–1106. [PubMed: 18666210]

Pak TR, Chung WC, Lund TD, Hinds LR, Clay CM, Handa RJ. The androgen metabolite, 5α-androstane-3β, 17β-diol (3β adiol), is a potent modulator of estrogen receptor-β1-mediated gene transcription in neuronal cells. Endocrinology. 2004; 146:147–155. [PubMed: 15471969]

Penatti, CAA.; Henderson, LP. Androgen actions on receptors and channels: Regulation of electrical excitability and synaptic transmission. In: Etgen, A.; Pfaff, D., editors. Molecular mechanisms of hormone action on behavior. New York: Academic Press; 2009. p. 153-182.

Pierce JP, Kurucz OS, Milner TA. Morphometry of a peptidergic transmitter system: Dynorphin b-like immunoreactivity in the rat hippocampal mossy fiber pathway before and after seizures. Hippocampus. 1999; 9:255–276. [PubMed: 10401641]

Pope HG Jr, Katz DL. Psychiatric and medical effects of anabolic-androgenic steroid use. A controlled study of 160 athletes. Arch Gen Psychiatry. 1994; 51:375–382. [PubMed: 8179461]

Qiao X, Suri C, Knusel B, Noebels JL. Absence of hippocampal mossy fiber sprouting in transgenic mice overexpressing brain-derived neurotrophic factor. J Neurosci Res. 2001; 64:268–276. [PubMed: 11319771]

Reddy DS. Anticonvulsant activity of the testosterone-derived neurosteroid 3α-androstanediol. Neuroreport. 2004a; 15:515–518. [PubMed: 15094514]

Reddy DS. Testosterone modulation of seizure susceptibility is mediated by neurosteroids 3α-androstanediol and 17β-estradiol. Neuroscience. 2004b; 129:195–207. [PubMed: 15489042]

Reddy DS. Neurosteroids: Endogenous role in the human brain and therapeutic potentials. Prog Brain Res. 2010; 186:113–137. [PubMed: 21094889]

Reddy DS, Jian K. The testosterone-derived neurosteroid androstanediol is a positive allosteric modulator of $GABA_A$ receptors. J Pharmacol Exp Ther. 2010; 334:1031–1041. [PubMed: 20551294]

Sakata K, Tokue A, Kawai N. Altered synaptic transmission in the hippocampus of the castrated male mouse is reversed by testosterone replacement. J Urol. 2000; 163:1333–1338. [PubMed: 10737539]

Salin PA, Scanziani M, Malenka RC, Nicoll RA. Distinct short-term plasticity at two excitatory synapses in the hippocampus. Proc Natl Acad Sci U S A. 1996; 93:13304–13309. [PubMed: 8917586]

Sarkey S, Azcoitia I, Garcia-Segura LM, Garcia-Ovejero D, DonCarlos LL. Classical androgen receptors in non-classical sites in the brain. Horm Behav. 2008; 53:753–764. [PubMed: 18402960]

Scharfman HE. Hyperexcitability in combined entorhinal/hippocampal slices of adult rat after exposure to brain-derived neurotrophic factor. J Neurophysiol. 1997; 78:1082–1095. [PubMed: 9307136]

Scharfman, HE. BDNF and the dentate gyrus mossy fibers: Implications for epilepsy. In: Stanton, PK.; Bramham, CR.; Scharfman, HE., editors. Synaptic plasticity and transynaptic signalling. New York: Springer Science and Business Media; 2005. p. 201-220.

Scharfman HE. The CA3 “backprojection” to the dentate gyrus. Prog Brain Res. 2007; 163:627–637. [PubMed: 17765742]

Scharfman HE, Maclusky NJ. Similarities between actions of estrogen and BDNF in the hippocampus: Coincidence or clue? Trends Neurosci. 2005; 28:79–85. [PubMed: 15667930]

Scharfman HE, MacLusky NJ. Estrogen and brain-derived neurotrophic factor (BDNF) in hippocampus: Complexity of steroid hormone-growth factor interactions in the adult cns. Front Neuroendocrinol. 2006; 27:415–435. [PubMed: 17055560]

Scharfman HE, Goodman JH, Sollas AL. Granule-like neurons at the hilar/CA3 border after status epilepticus and their synchrony with area CA3 pyramidal cells: Functional implications of seizure-induced neurogenesis. J Neurosci. 2000; 20:6144–6158. [PubMed: 10934264]

Scharfman HE, Smith KL, Goodman JH, Sollas AL. Survival of dentate hilar mossy cells after pilocarpine-induced seizures and their synchronized burst discharges with area CA3 pyramidal cells. Neuroscience. 2001; 104:741–759. [PubMed: 11440806]

Scharfman HE, Sollas AL, Smith KL, Jackson MB, Goodman JH. Structural and functional asymmetry in the normal and epileptic rat dentate gyrus. J Comp Neurol. 2002; 454:424–439. [PubMed: 12455007]

Scharfman HE, Mercurio TC, Goodman JH, Wilson MA, MacLusky NJ. Hippocampal excitability increases during the estrous cycle in the rat: A potential role for brain-derived neurotrophic factor. J Neurosci. 2003; 23:11641–11652. [PubMed: 14684866]

Scharfman HE, Hintz TM, Gomez J, Stormes KA, Barouk S, Malthankar-Phatak GH, McCloskey DP, Luine VN, Maclusky NJ. Changes in hippocampal function of ovariectomized rats after sequential low doses of estradiol to simulate the preovulatory estrogen surge. Eur J Neurosci. 2007; 26:2595–2612. [PubMed: 17970745]

Schjetnan AG, Escobar ML. In vivo BDNF modulation of hippocampal mossy fiber plasticity induced by high frequency stimulation. Hippocampus. 2010; 22:1–8. [PubMed: 20848610]

Scott R, Lalic T, Kullmann DM, Capogna M, Rusakov DA. Target-cell specificity of kainate autoreceptor and Ca2+-store-dependent short-term plasticity at hippocampal mossy fiber synapses. J Neurosci. 2008; 28:13139–13149. [PubMed: 19052205]

Shetty AK, Zaman V, Shetty GA. Hippocampal neurotrophin levels in a kainate model of temporal lobe epilepsy: A lack of correlation between brain-derived neurotrophic factor content and progression of aberrant dentate mossy fiber sprouting. J Neurochem. 2003; 87:147–159. [PubMed: 12969262]

Shimizu E, Hashimoto K, Okamura N, Koike K, Komatsu N, Kumakiri C, Nakazato M, Watanabe H, Shinoda N, Okada S, Iyo M. Alterations of serum levels of brain-derived neurotrophic factor

(BDNF) in depressed patients with or without antidepressants. Biol Psychiatry. 2003; 54:70–75. [PubMed: 12842310]

Skucas VA, Mathews IB, Yang J, Cheng Q, Treister A, Duffy AM, Verkman AS, Hempstead BL, Wood MA, Binder DK, Scharfman HE. Impairment of select forms of spatial memory and neurotrophin-dependent synaptic plasticity by deletion of glial aquaporin-4. J Neurosci. 2011; 31:6392–6397. [PubMed: 21525279]

Smith CC, Vedder LC, McMahon LL. Estradiol and the relationship between dendritic spines, NR2b containing NMDA receptors, and the magnitude of long-term potentiation at hippocampal CA3-CA1 synapses. Psychoneuroendocrinology. 2009; 34(Suppl 1):S130–142. [PubMed: 19596521]

Smith MD, Jones LS, Wilson MA. Sex differences in hippocampal slice excitability: Role of testosterone. Neuroscience. 2002; 109:517–530. [PubMed: 11823063]

Sohrabji F, Miranda RC, Toran-Allerand CD. Identification of a putative estrogen response element in the gene encoding brain-derived neurotrophic factor. Proc Natl Acad Sci U S A. 1995; 92:11110–11114. [PubMed: 7479947]

Spencer JL, Waters EM, Romeo RD, Wood GE, Milner TA, McEwen BS. Uncovering the mechanisms of estrogen effects on hippocampal function. Front Neuroendocrinol. 2008; 29:219–237. [PubMed: 18078984]

Stevens SJ, Harden CL. Hormonal therapy for epilepsy. Curr Neurol Neurosci Rep. 2011; 11:435–442. [PubMed: 21451944]

Tabori NE, Stewart LS, Znamensky V, Romeo RD, Alves SE, McEwen BS, Milner TA. Ultrastructural evidence that androgen receptors are located at extranuclear sites in the rat hippocampal formation. Neuroscience. 2005; 130:151–163. [PubMed: 15561432]

Tamura M, Koyama R, Ikegaya Y, Matsuki N, Yamada MK. K252a, an inhibitor of trk, disturbs pathfinding of hippocampal mossy fibers. NeuroReport. 2006; 17:481–486. [PubMed: 16543811]

Tamura M, Tamura N, Ikeda T, Koyama R, Ikegaya Y, Matsuki N, Yamada MK. Influence of brain-derived neurotrophic factor on pathfinding of dentate granule cell axons, the hippocampal mossy fibers. Mol Brain. 2009; 2:2. [PubMed: 19183490]

Tongiorgi E. Activity-dependent expression of brain-derived neurotrophic factor in dendrites: Facts and open questions. Neurosci Res. 2008; 61:335–346. [PubMed: 18550187]

Tyler WJ, Zhang XL, Hartman K, Winterer J, Muller W, Stanton PK, Pozzo-Miller L. BDNF increases release probability and the size of a rapidly recycling vesicle pool within rat hippocampal excitatory synapses. J Physiol. 2006; 574:787–803. [PubMed: 16709633]

Vierk R, Glassmeier G, Zhou L, Brandt N, Fester L, Dudzinski D, Wilkars W, Bender RA, Lewerenz M, Gloger S, Graser L, Schwarz J, Rune GM. Aromatase inhibition abolishes LTP generation in female but not in male mice. J Neurosci. 2012; 32:8116–8126. [PubMed: 22699893]

Wang JW, Dranovsky A, Hen R. The when and where of BDNF and the antidepressant response. Biol Psychiatry. 2008; 63:640–641. [PubMed: 18329441]

Wojtowicz T, Mozrzymas JW. Estradiol and GABAergic transmission in the hippocampus. Vitam Horm. 2010; 82:279–300. [PubMed: 20472144]

Xu B, Gottschalk W, Chow A, Wilson RI, Schnell E, Zang K, Wang D, Nicoll RA, Lu B, Reichardt LF. The role of brain-derived neurotrophic factor receptors in the mature hippocampus: Modulation of long-term potentiation through a presynaptic mechanism involving trkb. J Neurosci. 2000; 20:6888–6897. [PubMed: 10995833]

Yan Q, Rosenfeld RD, Matheson CR, Hawkins N, Lopez OT, Bennett L, Welcher AA. Expression of brain-derived neurotrophic factor protein in the adult rat central nervous system. Neuroscience. 1997; 78:431–448. [PubMed: 9145800]

Yeap BB. Testosterone and ill-health in aging men. Nat Clin Pract Endocrinol Metab. 2009; 5:113–121. [PubMed: 19165223]

Yoshino M, Sawada S, Yamamoto C, Kamiya H. A metabotropic glutamate receptor agonist DCG-IV suppresses synaptic transmission at mossy fiber pathway of the guinea pig hippocampus. Neurosci Lett. 1996; 207:70–72. [PubMed: 8710213]

Zivin, JA.; Bartko, JJ. Statistics for disinterested scientists. New York: Life Sciences; 1976.

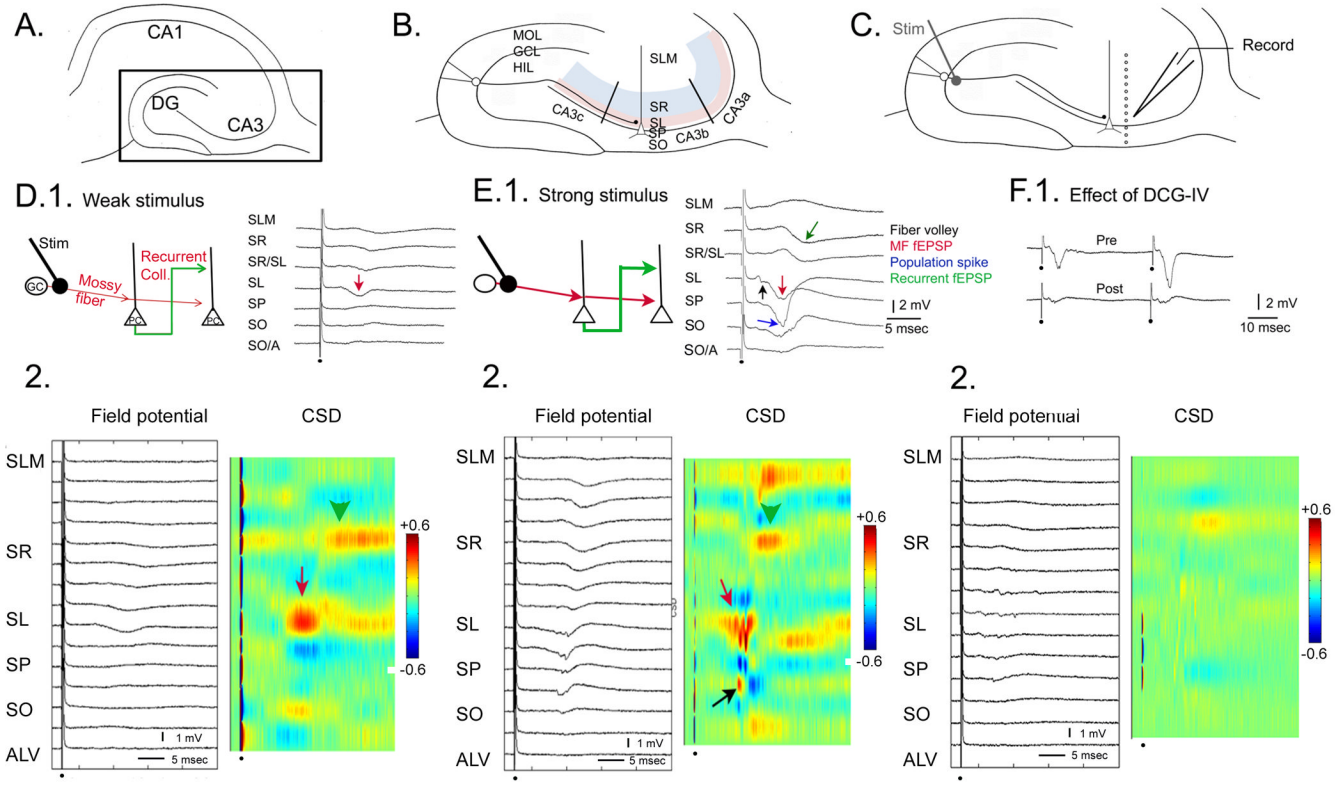

Figure 1. Methods to record mossy fiber-evoked fEPSPs (MF fEPSPs)

A. A diagram of the hippocampus in horizontal section.

B. The area outlined by the box in A is expanded to show the areas of the dentate gyrus and CA3 used in the experiments. SLM, stratum lacunosum-moleculare; SR, stratum radiatum (light blue); SL, stratum lucidum (light red); SP, stratum pyramidale; SO, stratum oriens. CA3a, b, c, are separated by lines reflecting divisions previously described (Lorente de Nó, 1934). The MF pathway is illustrated by a single granule cell and its main axon, terminating in stratum lucidum of area CA3. Granule cell mossy fibers also collateralize in the hilus (HIL). GCL= granule cell layer; MOL= molecular layer.

C. An illustration of the recording and stimulation sites. The stimulation site (stim) was the subgranular zone of the crest of the dentate gyrus. The recording site (record) was in CA3b. For current source density (CSD) analysis, recordings were made along an axis perpendicular to the cell layer (small circles indicate approximate recording sites).

D. 1. Left: A schematic illustrates the circuitry underlying responses elicited by low intensities of stimulation. Red arrows indicate the MF pathway; green arrows correspond to the recurrent collateral pathway.

Right: The red arrow shows that the predominant response to low intensity stimulation is a fEPSP recorded in stratum lucidum. In this figure and all others, the dots mark the stimulus artifacts, which are truncated.

2. A CSD analysis for the same slice using responses recorded from the alveus to stratum lacunosum-moleculare (Left). The CSD, shown on the right, illustrates that the primary current sink is in stratum lucidum (red arrow). This short latency current sink was followed by a longer latency sink in stratum radiatum (green arrowhead). Scale: +0.6 to −0.6 mV/mm^2.

E. 1. A schematic (on the left) illustrates the circuitry underlying the responses on the right, which were evoked with higher intensity of stimulation. The recurrent collateral pathway is activated more than part D because stronger stimuli led to suprathreshold activation of

pyramidal cells, indicated by the population spike (blue arrow). A fiber volley (black arrow) precedes the MF fEPSP recorded in stratum lucidum (red arrow). At a longer latency, a fEPSP was recorded in stratum radiatum (green arrow).

2. Left: Field potentials corresponding to higher stimulus strengths. Right: The CSD shows an early sink in stratum lucidum (red arrow) followed by a sink in the cell layer reflecting the population spike (blue arrow). Afterwards there is a sink in stratum radiatum (green arrow).

F. 1. Top: A representative recording of MF-evoked fEPSPs recorded in stratum lucidum in response to two identical stimuli, 40 msec apart, illustrating paired pulse facilitation, a characteristic of the MF pathway (Salin et al., 1996; Kamiya et al., 2002; Scott et al., 2008; Cosgrove et al., 2009). Bottom: Responses are decreased 30 min after exposure to 1 μM DCG-IV, an antagonist of MF transmission (Yoshino et al., 1996).

2. Field potentials and a CSD analysis of the same slice as E2, 30 min after adding 1 μM DCG-IV to the ACSF.

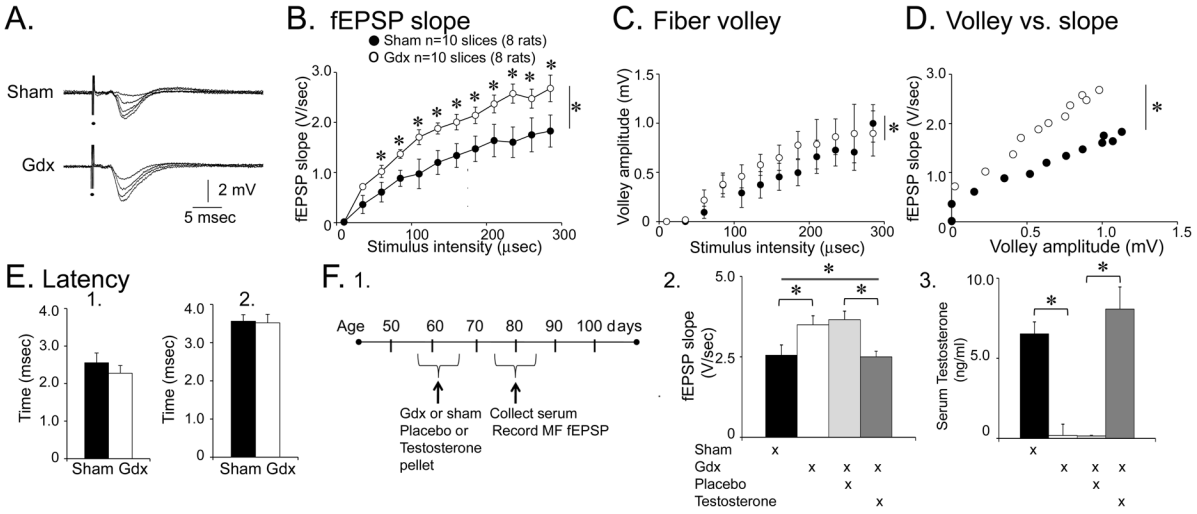

Figure 2. Slices from Gdx rats exhibit larger MF fEPSPs than sham rats

A. Representative examples of MF fEPSPs are shown for a sham (top) and Gdx rat (bottom) that had surgery approximately 2 weeks previously. The responses to a range of stimulus intensities are superimposed.

B. The input-output relation is shown for MF fEPSP slope from sham (black) and Gdx (white) rats. Gdx rats had significantly greater fEPSP slopes by two-way RMANOVA (asterisk to the right of the vertical bar indicate significance at the 0.05 level; asterisks above data points denote significance after post-hoc tests; for this and all other figures, all statistical comparisons are provided in the text).

C. The input-output relation is shown for fiber volleys from the same sham and Gdx rats. Differences were significant by ANOVA 4-parameter linear regression analysis ($p<0.001$).

D. MF fEPSP slope is plotted against fiber volley amplitude for the same data. The slopes were significantly different (asterisk; ANCOVA, $p<0.05$).

E. The mean latencies to 1) the onset of the fiber volley and 2) the onset of MF fEPSPs (evoked by a minimal stimulus) are shown; differences were not significant (Student's t-tests, $p>0.05$).

F. 1. A schematic illustrates the experimental timeline for Gdx rats that were implanted with a subcutaneous pellet containing testosterone or placebo. Comparisons were made to sham and Gdx rats that were untreated.

2. Comparison of MF fEPSP slope showed group differences (asterisk over the bar, one-way ANOVA; $p<0.05$). Gdx rats that were untreated (white) had significantly greater fEPSP slopes than sham rats that were untreated (black; asterisk over the bracket; post-hoc test, $p<0.05$); Gdx rats treated with placebo (light grey) had significantly greater fEPSP slopes than Gdx rats treated with testosterone (dark grey; asterisk over the bracket; post-hoc test, $p<0.05$). fEPSPs in slices of Gdx rats treated with testosterone were similar to sham rats; Gdx rats that were treated with placebo (dark grey) were similar to Gdx rats that were untreated (white; post-hoc tests, $p>0.05$).

3. ELISA showed that serum testosterone levels were at the lower limit of the assay for placebo and untreated Gdx rats. Differences between sham rats and Gdx rats treated with testosterone were not significant (Kruskal Wallis ANOVA, followed by post-hoc test, $p>0.05$), suggesting that testosterone administration restored testosterone levels to a comparable range as sham rats. Differences between untreated sham and untreated Gdx rats were significant; differences between Gdx rats treated with placebo and Gdx rats treated with testosterone were also significant (asterisks above the brackets; Kruskal Wallis ANOVA followed by post-hoc tests, $p<0.05$)

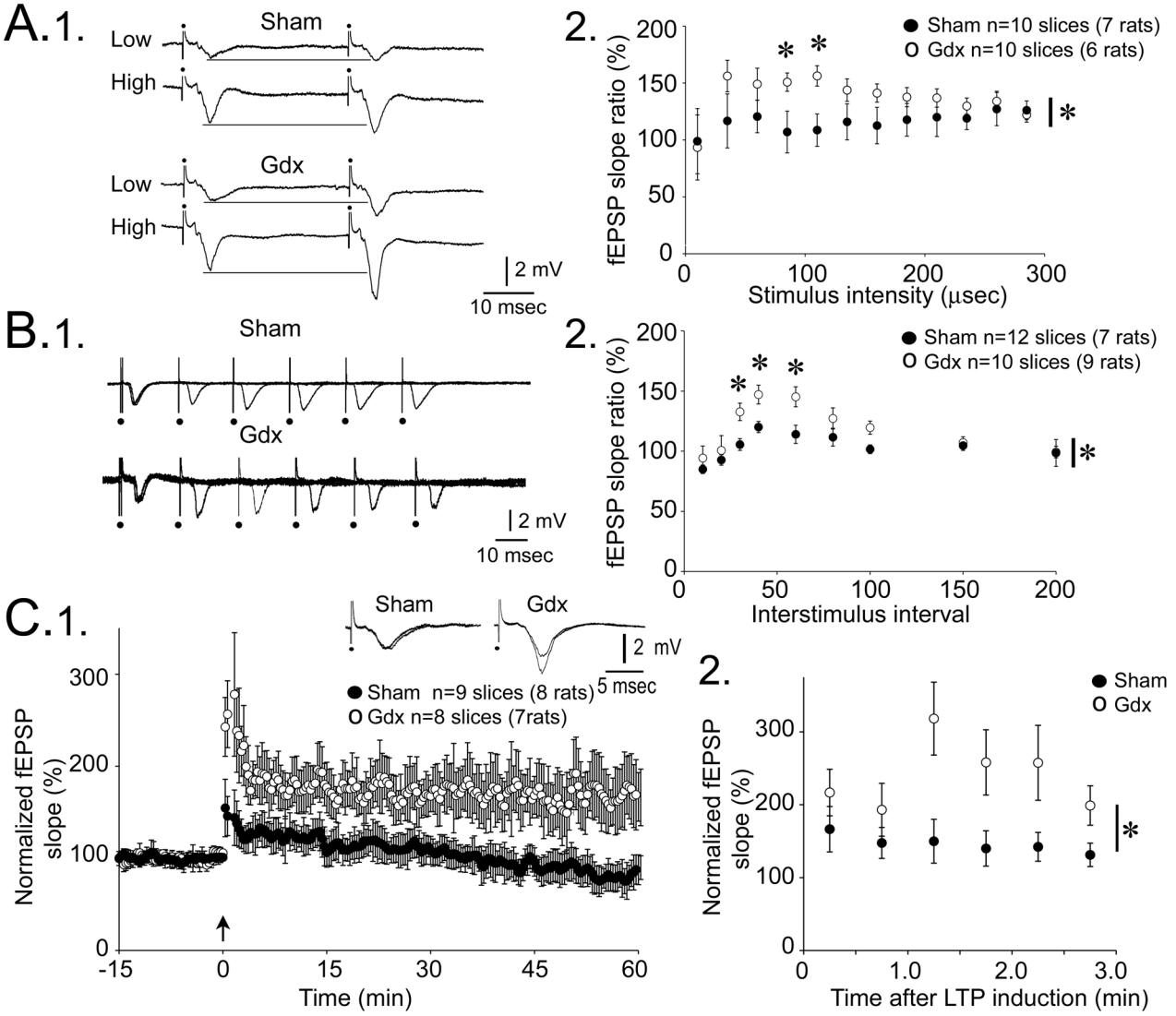

Figure 3. Increased PPF, PTP and LTP in Gdx rats compared to sham controls

A. 1. MF fEPSPs elicited by low or high stimulus strengths (35 μsec or 110 μsec) are shown for a sham (top) and Gdx (bottom) rat. Horizontal lines are shown to facilitate comparisons.

2. Mean PPF was significantly greater in Gdx rats compared to sham rats when the stimulus strength was intermediate. In A–B, the asterisk beside the vertical bar indicates $p<0.05$ for a main effect of Gdx on PPF by two-way RMANOVA; the asterisks above the symbols denote $p<0.05$ for post-hoc tests.

B. 1. Examples of PPF recorded from a slice of a Gdx and sham rat. In each case, responses are superimposed, each using a half-maximal stimulus and 20–100 msec interstimulus intervals.

2. Mean PPF was greater in Gdx rats by two-way RMANOVA (asterisk by the vertical bar, $p<0.05$) followed by post-hoc tests ($p<0.05$) for the 30–60 msec interstimulus intervals (asterisks above the symbols).

C. 1. Normalized fEPSP slope measurements are shown for slices from Gdx rats (white circles) and sham (black circles) before and after LTP induction (two 25 Hz, 1 sec trains, 10 sec apart, at the arrow). There was greater LTP in Gdx rats (Student's t-test at 60 min after LTP induction; $p<0.05$).

2. PTP over the first three minutes after LTP induction was greater in slices from Gdx rats compared to sham rats (asterisk; two-way RMANOVA, $p<0.05$).

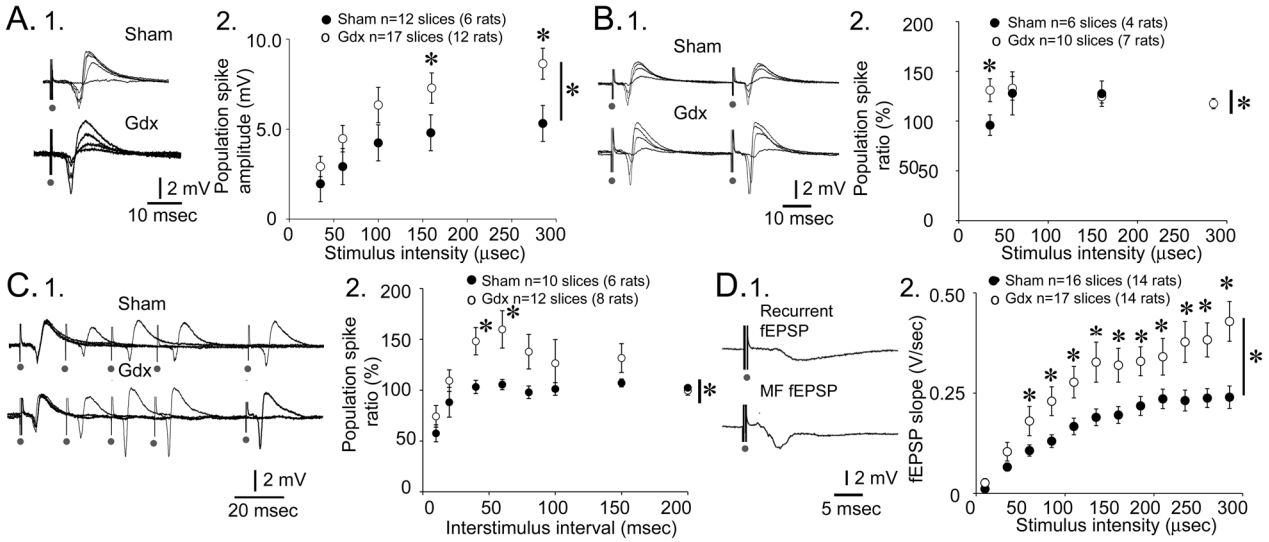

Figure 4. Larger population spikes and greater recurrent fEPSPs in Gdx rats compared to sham rats

A. 1. Superimposed responses to MF stimulation recorded in stratum pyramidale.

2. An input-output curve for population spike amplitude shows that amplitudes were greater in Gdx rats (two-way RMANOVA; $p<0.05$; asterisk by the vertical bar). Significance of post-hoc tests is denoted by asterisks above the symbols.

B. 1. PPF in a slice from a sham and Gdx rat. PPF was elicited using many stimulus strengths and a constant (40 msec) interstimulus interval.

2. Mean PPF was greater in Gdx rats at the lowest stimulus intensities (asterisks).

C. Representative examples (1) and quantification (2) of PPF of population spike amplitude using a half-maximal stimulus strength and a range of interstimulus intervals (10–200 msec). PPF was greater in Gdx rats at the 40 and 60 msec intervals (asterisks).

D. 1. A representative response in stratum radiatum (top) and stratum lucidum (bottom) to the same MF stimulus shows the longer latency of the response recorded in stratum radiatum, which we interpret to be a disynaptic fEPSP mediated by recurrent collaterals of pyramidal cells (see Figure 1).

2. Recurrent fEPSP slope was greatest in slices from Gdx rats (asterisks).

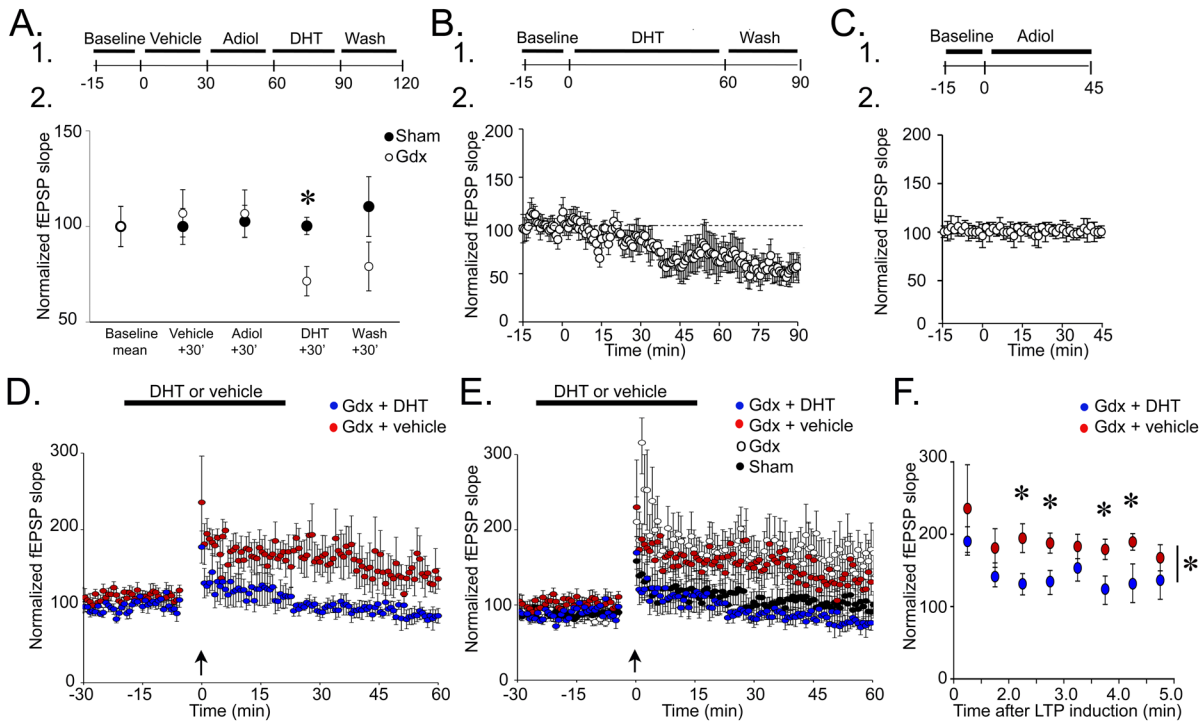

Figure 5. DHT-sensitivity of MF transmission and LTP in Gdx rats

A. 1. A diagram of the experimental timeline is shown. Slices from Gdx rats (white circles, n=4 slices, 4 rats) and sham rats (n=3 slices, 3 rats) were exposed to vehicle (0.0005% ethanol) for 30 min and then 50 nM 5α-androstane-3α,17β-diol (Adiol) for 30 min, followed by 50 nM DHT and then wash.

2. MF fEPSP slopes decreased after exposure to DHT in Gdx rats (asterisk; one-way RMANOVA followed by post-hoc tests, $p<0.05$) but not sham rats (one-way RMANOVA, $p>0.05$).

B. 1. The experimental procedure is shown. Slices from Gdx rats (n=4 slices, 4 rats) were exposed to 50 nM DHT immediately after a 15 min baseline.

2. fEPSP slope decreased during exposure to DHT and the effect persisted after wash.

C. 1. The experimental procedure is shown. After a 15 min baseline period, slices from Gdx rats (n=5 slices, 5 rats) were exposed to 50 nM Adiol for 45 min.

2. The results of the experiment diagrammed in C1 shows that there was no detectable effect.

D. Slices from Gdx rats were treated (designated by the horizontal bar) with 50 nM DHT (blue circles, n=5 slices, 5 rats) or vehicle (red circles, n=8 slices, 8 rats) for 15 min before and after LTP induction (at the arrow). There was greater LTP (measured 60 min after LTP induction) in DHT-treated slices compared to vehicle (Student's t-tests, $p<0.05$).

E. The results from D are superimposed on the results of untreated Gdx rats (white circles) and sham rats (black circles; data from Figure 3). There were no significant differences in LTP between DHT-treated slices and untreated sham controls (Student's t-test, $p>0.05$).

F. The first minutes after LTP induction in D and E are expanded for slices from Gdx rats treated with DHT (blue circles) and Gdx rats treated with vehicle (red circles). The differences were significant (asterisk beside the vertical bar, two-way RMANOVA, $p<0.05$; asterisks above the symbols, post-hoc tests, $p<0.05$).

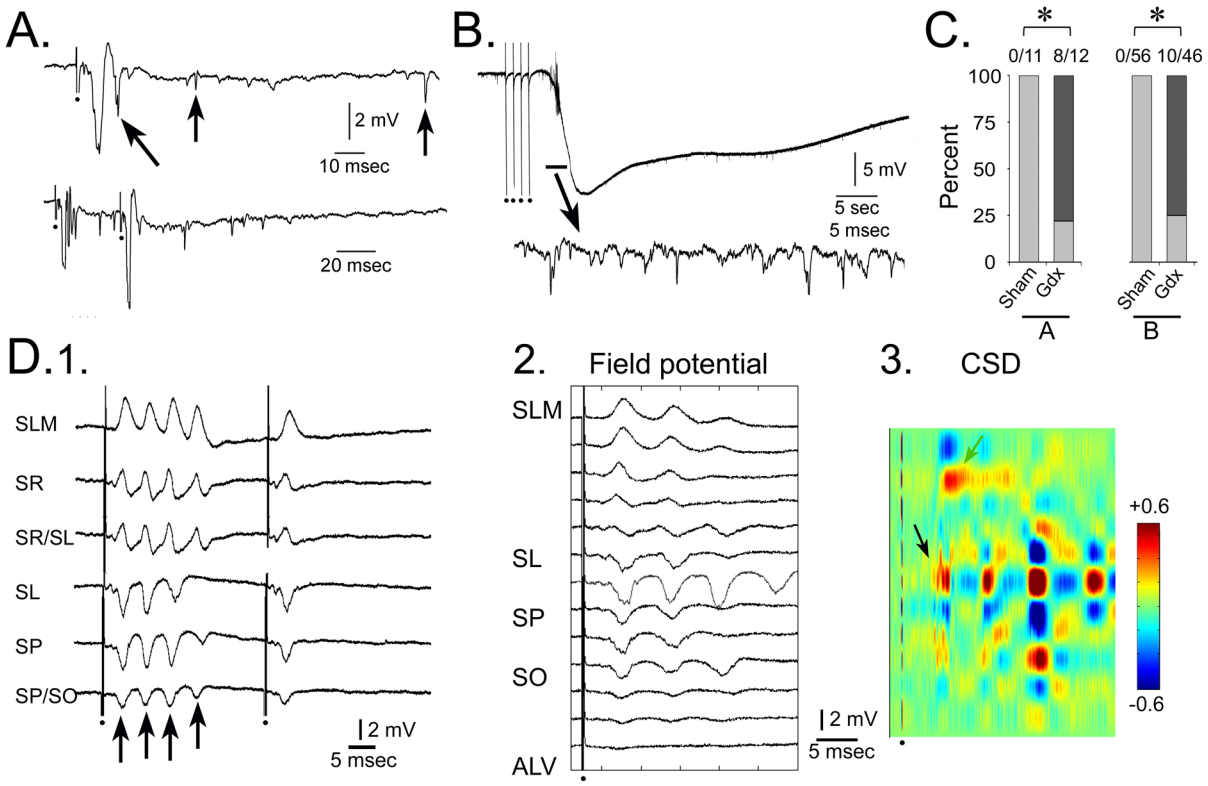

Figure 6. Increased excitability in area CA3 of Gdx rats

A. An example of a response to MF stimulation in a slice from a Gdx rat, recorded in stratum pyramidale, shows that more than one population spike (angled arrow) was elicited by a single stimulus, an indication of increased excitability. In addition, spontaneous activity was higher than normal (vertical arrows denote unit activity and spontaneous field potentials).

B. Top: An example of a spreading depression (SD) episode in a slice from a Gdx rat. Repetitive MF stimuli (half-maximal stimuli in pairs with 40 msec interstimulus intervals at 1 Hz for a total of 8 stimuli in 4 sec) induced SD. In other slices, TBS elicited SD (see part C). Bottom: The part of the SD episode marked by the horizontal bar is expanded to show the increase in spontaneous activity at the onset of SD.

C. Incidence of hyperexcitability in slices from Gdx rats is shown.

Left (corresponding to 6A): More than one field potential per MF stimulus occurred in 0/56 slices from sham rats and 10/46 slices (22%) from Gdx rats.

Right (corresponding to 6B): SD episodes were evoked by TBS stimulation in 0/11 slices from sham rats and 8/12 (75%) of slices from Gdx rats which was a significant difference (asterisks; χ^2 test for A; Fisher's test for B, $p<0.05$).

D. Rhythmic, repetitive field potentials in a subset of slices from Gdx rats.

1. A fixed stimulus to the MFs was used to examine responses in all layers of area CA3b. The number of repetitive field potentials (arrows) was similar regardless of the layer. The largest fEPSP occurred in stratum lucidum with reversal of polarity in stratum lacunosum-moleculare. A second stimulus triggered 40 msec after the first only elicited one field potential.

2–3. CSD analysis of the response to the first stimulus illustrates the stereotypical nature of repetitive field potentials and their ability to induce abnormal sinks and sources throughout area CA3. An arrow points to the sink with shortest latency, in stratum lucidum. Scale: +0.6 to −0.6 mV/mm^2.

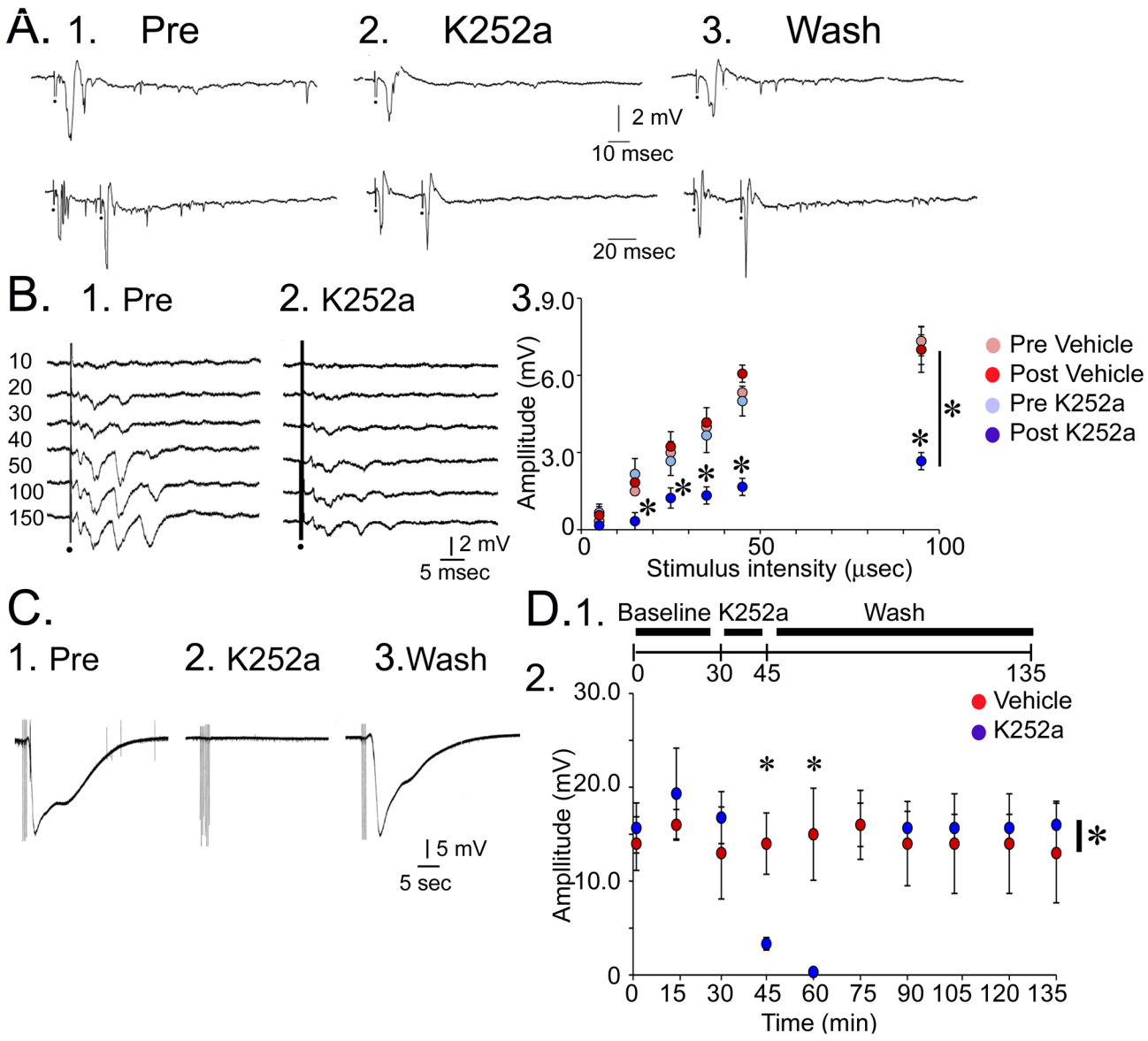

Figure 7. K252a reduces excitability in slices from Gdx rats

A. 1. The response to MF stimulation is shown before 300 nM K252a was added to the ACSF. Same slices as Figure 6A.

2. The response to the same stimulus is shown 45 min later. The population spikes evoked by the stimulus, especially the secondary population spikes, were reduced by K252a. Spontaneous activity was also reduced.

3. There was a partial reversal after K252a-containing ACSF was replaced by drug-free buffer for 60 min.

B. 1–2. K252a was perfused onto a different slice from a Gdx rat where rhythmic, repetitive field potentials were evoked (same slice as Figure 6D). Several stimulus strengths (10–150 µsec) were used before (1, Pre) and after K252a application (10–150 µsec; 2, K252a). K252a reduced the amplitude of evoked responses.

3. The amplitude of the first fEPSP recorded in stratum lucidum is shown for all stimulus intensities. In addition, data from slices treated with vehicle are shown. There was a

significant effect of K252a (comparison of pre-K252a and 30 min post-K252a; light blue and dark blue circles, two-way RMANOVA followed by post-hoc tests, asterisks indicate $p<0.05$) but there were no effects of vehicle (comparison of pre-DMSO and 30 min post-DMSO; light red and dark red circles; two-way RMANOVA; $p>0.05$).

C. K252a blocked spreading depression episodes reversibly.

1. An example if an SD episode in response to repetitive MF stimulation (2 half-maximal stimuli 40 msec apart at 1 Hz for 10 sec) is shown before adding 300 nM K252a to the buffer.

2. After K252a, the same stimulation did not evoke SD.

3. Sixty min after drug-free buffer was resumed, stimulation evoked SD.

4. A timeline of the experiments is shown. MF stimulation (the same stimulus train as in C1–3) was triggered at 15 min intervals during a baseline, followed by exposure to 300 nM K252a (or vehicle) for 15 min, and drug-free ACSF at the end.

5. A comparison of the effects of vehicle and K252a on the amplitude of SD episodes evoked by repetitive 1 Hz MF stimulation in slices from Gdx rats (n=3 slices, 3 rats/treatment). Two-way RMANOVA showed that there was a significant effect of K252a compared to vehicle (asterisk by the vertical bar); one-way RMANOVA followed by post-hoc tests showed a significant effect of K252a 15 and 30 min after the start of K252a application (asterisks above symbols, $p<0.05$).

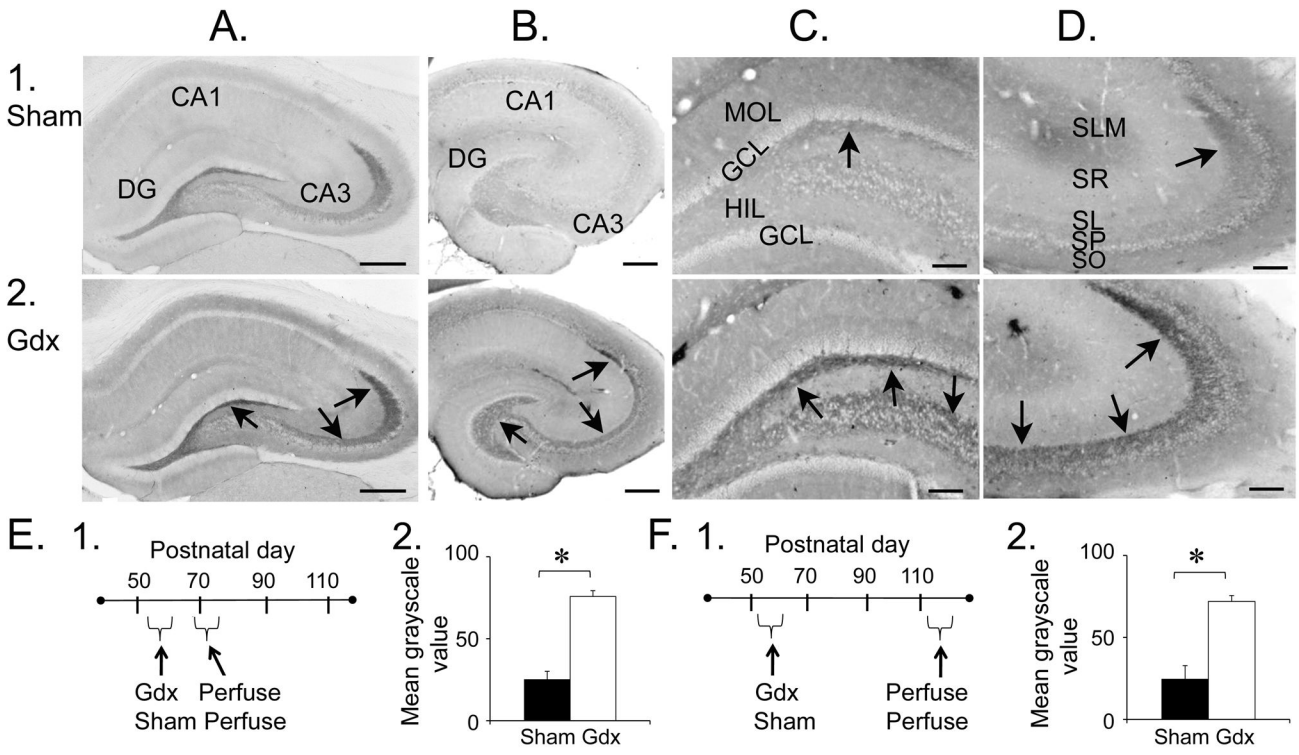

Figure 8. Gdx rats exhibit increased BDNF-ir in the MF pathway

A. BDNF-ir in a sham (1) and Gdx rat (2) using a rabbit polyclonal antibody to BDNF (provided by Amgen-Regeneron Partners). DG=dentate gyrus. Arrows point to the MF pathway. Calibration = 500 μm.

B. BDNF-ir in a different sham (1) and Gdx (2) rat using a different antibody (mouse monoclonal; Sigma-Aldrich). Calibration = 500 μm.

C. Higher magnification of a coronal section from the same animals as in 8B. There was greater BDNF-ir in the MFs (arrows) of the Gdx rat. MOL = molecular layer. GCL = granule cell layer. HIL = hilus. Calibration = 100 μm.

D. Area CA3 of the same sections used in 8C show MF staining (arrows) that is darker in the Gdx rat. Calibration same as C.

E. 1. A timeline is shown for experiments where rats were subjected to surgery at approximately 60 days of age and perfusion-fixed approximately 2 weeks later.

2. Mean gray scale values (measured as described in Figure 9H1). Sections from Gdx rats exhibited greater values than sham rats (asterisk, Student's t-tests, $p<0.05$).

F. 1. The timeline is shown for experiments where rats had surgery at approximately 60 days of age, and were perfused approximately 2 months later.

2. Sections from Gdx rats had greater values than sham rats (asterisk, Student's t-test, $p<0.05$).

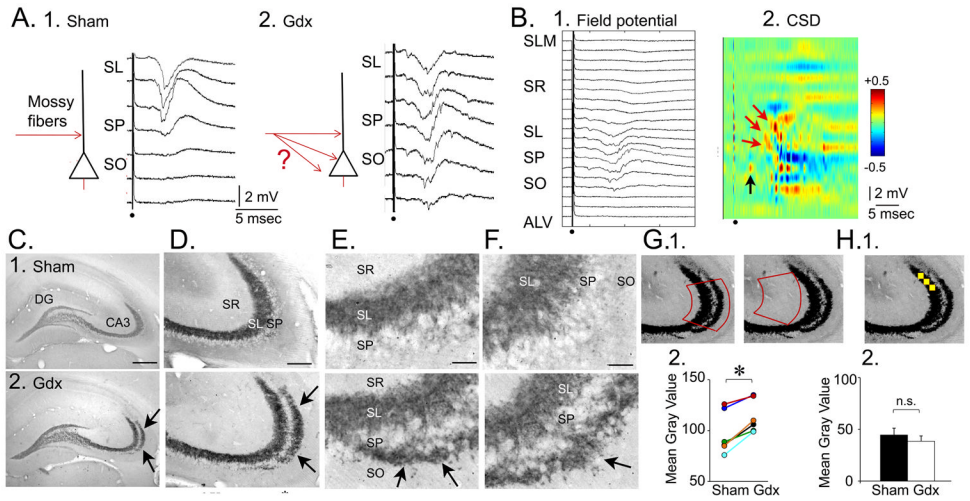

Figure 9. Gdx in adult male rats leads to MF sprouting in stratum oriens of CA3a/b

A. 1. Left: A schematic illustrates the MF pathway (red) in a sham rat. Right: Representative responses to a fixed MF stimulus are shown for a slice of a sham rat. For A1–2, only those responses between stratum lucidum and stratum oriens are shown.

2. Left: An illustration of the MF pathway in a Gdx rat where MFs may sprout into stratum oriens (red arrows with question mark). Right: Responses of a slice from a Gdx rat recorded in a similar manner to A1. Responses are similar in stratum lucidum, pyramidale and oriens and appear to be fEPSPs.

B. All field potentials (1) and CSD (2) are shown for the Gdx rat in A2. Red arrows point to current sinks in or near stratum lucidum. The black arrow corresponds to a fiber volley in stratum oriens, suggesting that MF axons were present in stratum oriens.

C–F. Dynorphin-ir in a sham (1) and Gdx (2) rat. Arrows in D–F point to the area of stratum oriens where dynorphin-ir is evident in the Gdx rat but not the sham rat. DG = dentate gyrus; SR = stratum radiatum; SL = stratum lucidum; SP = stratum pyramidale; SO = stratum oriens. Calibration (C) = 500 μm. Calibration (D) = 100 μm. Calibration (E–F) = 25 μm.

G. 1. Left: The template (red) that was used to measure dynorphin-ir in CA3 is shown. Right: To estimate background staining, the template was positioned over stratum radiatum as shown. For each section, the mean gray scale value for the background was subtracted from the mean gray scale value of the first measurement.

2. Animals were prepared in pairs (same surgery date, same perfusion date, immunocytochemical processing at the same time) and results are shown for each pair (left, sham; right, Gdx). The Gdx rats exhibited a greater mean gray scale value (asterisk; Paired t-test; $p<0.05$).

H. 1. The yellow box that was used to determine mean gray scale values of the terminal field of MFs is shown. Three measurements within the area of the terminal plexus, depicted by three boxes, were averaged for each section. Three measurements in stratum radiatum were also made, to estimate background staining, and the mean of these measurements were subtracted from the mean of the stratum lucidum measurements for H2.

2. The mean gray scale value was similar in sham and Gdx rats (n.s.; Paired t-test, $p>0.05$). The results suggest that dynorphin-ir in stratum oriens of Gdx rats was due to new dynorphin-ir fibers, not increased dynorphin-ir in pre-existing fibers.

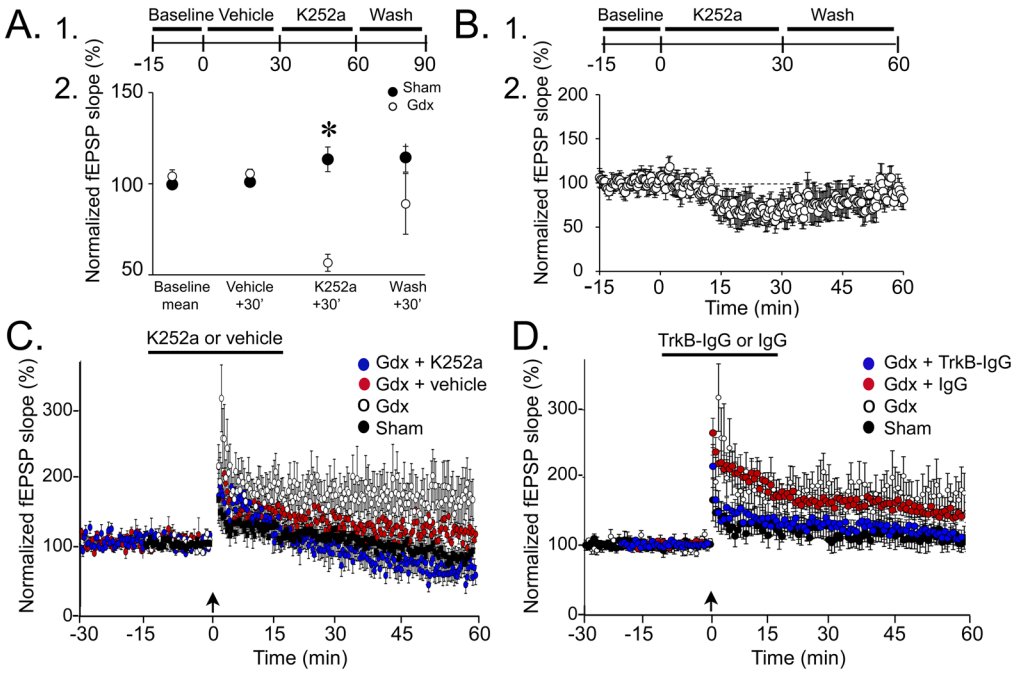

Figure 10. K252a reduces MF transmission and LTP in Gdx rats but not sham controls

A. 1. The experimental procedure is diagrammed. Slices from Gdx rats (white circles; n=4 slices, 4 rats) or sham rats (black, n=4 slices, 4 rats) were exposed to vehicle (0.003% DMSO) for 30 minutes and then 300 nM K252a followed by drug-free ACSF.

2. MF fEPSP slopes in Gdx rats decreased when exposed to K252a (asterisk, one-way RMANOVA followed by post-hoc tests, $p<0.05$) but there was no effect in sham rats (one-way RMANOVA, $p>0.05$).

B. 1. The experimental procedure is shown. Slices from Gdx rats (8 slices, 8 rats) were perfused with 300 nM K252a for 30 minutes and then returned to drug-free buffer.

2. Normalized MF fEPSP slope is plotted for all slices. K252a reduced fEPSP slope and there was recovery with wash.

C. Slices from Gdx rats were tested for 15 min to establish a stable baseline and then pretreated with 300 nM K252a for 15 min (blue circles; 7 slices, 5 rats) or vehicle (red circles; 9 slices, 6 rats) and then the trains to induce LTP were triggered (arrow). After 15 minutes, perfusion with drug-free ACSF resumed. There was greater LTP in slices from Gdx rats treated with vehicle compared to Gdx rats treated with K252a (measured 60 min after LTP induction, Student's t-test, $p<0.05$). For comparison, the results of experiments that used untreated slices from Gdx rats (white circles) and untreated slices from sham rats (black circles) are shown (from Figure 3).

D. After a 15 min-long baseline, slices from additional Gdx rats were exposed to 1 ng/ml TrkB-IgG for 10 min (blue circles; 7 slices, 6 rats) or control IgG (1 ng/ml; red circles; 9 slices, 6 rats). After LTP induction, TrkB-IgG or IgG were continued for 10 min. Then drug-free buffer was reinstated. Data from slices that were from untreated Gdx rats (white circles) and untreated slices from sham rats (black circles) are also shown, as for C. Slices from Gdx rats that were treated with TrkB-IgG were not statistically different from untreated slices from sham rats at 60 min following LTP induction (Student's t-test, $p<0.05$). Slices from Gdx rats that were treated with vehicle were not different from untreated Gdx rats (Student's t-test, $p<0.05$). The results suggest that a Trk-sensitive form of LTP emerged after Gdx.